

This is the author's manuscript for publication. The publisher-formatted version may be available through the publisher's web site or your institution's library.

## Dynamic factor analysis of surface water management impacts on soil and bedrock water contents in Southern Florida Lowlands

I. Kisekka, K. W. Migliaccio, R. Muñoz-Carpena, B. Schaffer, Y. C. Li

### How to cite this manuscript

If you make reference to this version of the manuscript, use the following information:

Kisekka, I., Migliaccio, K. W., Muñoz-Carpena, R., Schaffer, B., & Li, Y. C. (2013). Dynamic factor analysis of surface water management impacts on soil and bedrock water contents in Southern Florida Lowlands. Retrieved from <http://krex.ksu.edu>

### Published Version Information

**Citation:** Kisekka, I., Migliaccio, K. W., Muñoz-Carpena, R., Schaffer, B., & Li, Y. C. (2013). Dynamic factor analysis of surface water management impacts on soil and bedrock water contents in Southern Florida Lowlands. *Journal of Hydrology*, 488, 55-72.

**Copyright:** © 2013 Elsevier B.V.

**Digital Object Identifier (DOI):** doi:10.1016/j.jhydrol.2013.02.035

**Publisher's Link:** <http://www.sciencedirect.com/science/article/pii/S0022169413001583>

This item was retrieved from the K-State Research Exchange (K-REx), the institutional repository of Kansas State University. K-REx is available at <http://krex.ksu.edu>



27 contents in terms of regression coefficient magnitude was canal stage. Based on DFA results, a simple  
28 regression model was developed to predict soil and bedrock water contents at various elevations as a  
29 function of canal stage and net recharge. The performance of the simple model ranged from good ( $C_{eff}$   
30 ranging from 0.56 to 0.74) to poor ( $C_{eff}$  ranging from 0.10 to 0.15), performance was better at sites with  
31 smaller depths to water table ( $< 1$  m) highlighting the effect of micro-topography on soil and bedrock  
32 water content dynamics. Assessment of the effect of 6, 9 and 12 cm increases in canal stage using the  
33 simple regression model indicated that changes in temporal variation in soil and bedrock water contents  
34 were negligible (average  $< 1.0\%$  average change) at 500 to 2000 m from C111 (or low elevations) which  
35 may be attributed to the near saturation conditions already occurring at these sites. This study used DFA  
36 to explore the relationship between soil and bedrock water dynamics and surface water stage in shallow  
37 water table environments. This approach can be applied to any system in which detailed physical  
38 modeling would be limited by inadequate information on parameters or processes governing the physical  
39 system.

40 **Key words:** Soil water content, bedrock water content, scaled frequency, Dynamic Factor Analysis, canal  
41 stage, water table

42 Abbreviations: DFA, dynamic factor analysis; SF, scaled frequency;  $R_{net}$ , net surface recharge; MWT,  
43 mean water table elevation; S177T, C111 canal stage; SFWMD, South Florida Water Management  
44 District; AIC, Akaike information criterion; BIC, Bayesian information criterion; VIF, variance inflation  
45 factor; NGVD29, National Geodetic Vertical Datum of 1929.

46

47 **1. Introduction**

48 In an attempt to correct some of the undesired consequences of south Florida's extensive drainage  
49 canal network on the region's ecosystem, an environmental restoration project named the Comprehensive  
50 Everglades Restoration Plan (CERP) is currently under implementation. CERP was approved by the  
51 United States Congress under the Water Resources Development Act (2000). One of the 68 components  
52 that comprise CERP is the C111 spreader canal project whose goal is to reduce the impacts of C111 (i.e.,  
53 reduce groundwater seepage into C111) on Everglades National Park (ENP) and Taylor Slough which is a  
54 natural drainage feature that conveys water to Florida while maintaining existing levels of flood  
55 protection in the adjacent agricultural and urban areas (U.S. Army Corps of Engineers [USACP] and  
56 South Florida Water Management District [SFWMD], 2009). As part of the C111 spreader canal project,  
57 structural modifications and operational adjustments involving incremental raises in canal stage are  
58 planned along one of the major canals (i.e., C111) separating ENP and agricultural production areas to the  
59 east of the canal. The increase in canal stage will occur by changing surface water management at the  
60 gated spillway located at structure named S18C (Fig. 1) in the form of incremental raises in canal stage of  
61 up to 12 cm.

62 It is anticipated that the planned rise in C111 canal stage will affect water table levels in the adjacent  
63 agricultural areas. Earlier research indicated that there is substantial interaction between the highly  
64 permeable Biscayne aquifer and water level in canals (Genereux and Slater, 1999). The hydraulic  
65 connection between Biscayne aquifer and canal C111 causes the shallow water table system to fluctuate  
66 with respect to changes in canal stage. Using the drain to equilibrium assumption, Barquin et al. (2011)  
67 showed that water table elevation in the Biscayne aquifer significantly influenced soil and bedrock water  
68 contents in a fruit orchard with soil and bedrock formations that are very similar to our current study site.  
69 Therefore, raising water table elevation could result in increased soil and bedrock water contents or  
70 greater saturation of the root zone which could affect the production of winter vegetables predominately  
71 grown in this area. Saturation of the root zone could impact yield potential by impairing root growth due

72 to anoxia, reducing stomatal conductance, and reducing net CO<sub>2</sub> assimilation (Schaffer, 1998). In addition  
73 to physiological stress, having the soils saturated could render movement of machinery difficult and also  
74 impact growing season and market dates. However, it is not known to what extent the proposed structural  
75 modifications and operational adjustments along canal C111 would impact water table elevations and thus  
76 soil and bedrock water contents in agricultural areas east of the canal.

77 Vegetable production in Miami-Dade County, a substantial proportion of which is located along the  
78 extensive eastern boundary of ENP, is a significant contributor to both the local and state economies.  
79 According to the 2007 Census of Agriculture from the US Department of Agriculture (USDA, 2007), the  
80 total value of vegetables produced in Miami-Dade County was over 128 million dollars in 2007. Green  
81 beans, sweet corn, squash, tomatoes and sweet potato are the dominant vegetables grown in the area.  
82 There is need to quantify the impacts of hydrological modifications and surface water management on  
83 agricultural land use at field scale because large regional hydrology models have discretization that might  
84 not be suitable for resolving small scale micro-topographic differences within the landscape.

85 Long term monitoring and exploratory analysis of soil and limestone bedrock water contents could  
86 characterize the effect of various drivers on the temporal variability of water contents. The soils in the  
87 agricultural areas east of C111 were created from scarification of the underlying limestone bedrock hence  
88 they are very shallow and have high gravel content. Three main stresses that influence soil water content  
89 that could be included in exploratory analysis are 1) canal stage, which affects water table elevation; 2)  
90 rainfall, and 3) evapotranspiration. While these stresses may be assessed using physically based models of  
91 vadose zone flow and transport, implementation of unsaturated flow models (e.g., WAVE [Vanclooster  
92 et al., 1995] or HYDRUS [Šimůnek, et al., 2008]) is not an easy task since they contain numerous  
93 parameters and processes that have to be quantified (Ritter et al., 2009). In very gravelly and shallow soils  
94 such as those in south Miami-Dade County, quantifying parameters such as hydraulic conductivity for use  
95 in Richards' equation is further complicated by having porous gravelly soils that are not homogeneous.  
96 Previous applications of WAVE, for example, in gravelly soils of south Florida have indicated that a

97 detailed description of soil hydraulic properties (e.g., using dual porosity) could result in improved  
98 robustness of vadose zone models (Duwig et al., 2003; Muñoz-Carpena et al., 2008). Therefore the  
99 success of applying physically based models to simulate soil and bedrock water dynamics depends largely  
100 on proper conceptualization of location specific processes and proper measurement or estimation of  
101 parameters. In this context, complementary exploratory tools such as Dynamic Factor Analysis (DFA)  
102 which are not processes based are desired as simpler preliminary exploratory tools that could also be used  
103 for preliminary predictions of the impact of surface water management decisions on land use.

104 A comprehensive description of DFA and modeling can be found in Zuur et al. (2003). For purposes  
105 of aiding discussion, we only provide a brief description of this technique. DFA is a dimension reduction  
106 multivariate time series analysis technique that is used to estimate underlying common patterns (common  
107 trends) in short time series as well as the effect of explanatory variables on response variables. The  
108 advantage of DFA over other traditional dimensional reduction techniques (e.g., Factor Analysis or  
109 Principal Component Analysis) is that DFA accounts for the time component. This allows the underlying  
110 hidden effects driving the temporal variation in the observed time series data to be detected (Zuur et al.,  
111 2003). DFA does not require observed time series to be long and stationary. Although non-stationarity  
112 could be handled through de-trending, trends in the times series could hold necessary information  
113 required to explain the temporal dynamics in the observed variable (Ritter et al., 2009). In addition, DFA  
114 can handle missing values in the observed time series (i.e., DFA does not require data sets to be regularly  
115 spaced). Missing values in observed time series data sets are not uncommon especially when time series  
116 data are obtained from unattended automatic data logging field instruments (e.g., multi-sensor capacitance  
117 probes for soil water monitoring).

118 DFA applications are documented in literature from several disciplines (e.g., Geweke, 1977; Márkus  
119 et al., 1999; Zou and Yu, 1999; Zuur et al., 2003; Zuur and Pierce, 2004; Muñoz-Carpena et al., 2005;  
120 Ritter and Muñoz-Carpena, 2006; Zuur et al., 2007; Ritter et al., 2009; Kaplan et al., 2010a; Kaplan and  
121 Muñoz-Carpena, 2011). Thus, we only provide a brief review of the most relevant examples. Ritter and

122 Muñoz-Carpena (2006) applied DFA and modeling to study interactions between surface water and  
123 groundwater levels within the Frog Pond agricultural area located west of canal C111 in south Florida  
124 (Fig.1). Their results indicated that the two canals surrounding the Frog Pond area had the greatest  
125 influence on temporal changes in water table elevation. Their study did not address the issue of the impact  
126 of surface management decisions on soil water content. Soil water is a major concern for vegetable  
127 growers in south Florida due to the impact saturated or near saturated soil conditions have on planting  
128 dates and yield losses (Fig. 1).

129 Others have applied DFA and modeling to study soil water dynamics. Ritter et al. (2009) applied  
130 DFA to analyze temporal changes in soil water status of a humid, subtropical, evergreen forest in Canary  
131 Islands, Spain. Kaplan and Muñoz-Carpena (2011) applied DFA to study the complementary effects of  
132 surface and groundwater on soil water dynamics in a coastal flood plain. Thus, DFA was successfully  
133 used to identify unexplained variability in observed hydrologic time series and to assess the effect of  
134 selected explanatory variables on response variables (observed time series of interest).

135 The difference between our study and prior studies is that we applied DFA to investigate the effect of  
136 surface water management in canals on soil water dynamics in an agricultural area with very shallow very  
137 gravely loam soils, and unlike in the previous studies we also considered not only the effects of potential  
138 evaporation ( $ET_0$ ) but also the effect of water table evaporation given the shallow water table. We then  
139 attempted to develop a simple model, using information from the DFA, to predict soil water content from  
140 easily measured variables such as canal stage and recharge (i.e., difference between rainfall and  
141 evapotranspiration). Canal stage was selected instead of water table elevation since water table elevation  
142 data in our study area are less complete due to the limited period of record and the limited number of  
143 continuously monitored groundwater wells. Canal stage has been monitored for a longer period of record  
144 and has no foreseeable end of data collection, thus it is a more reliable measurement for long-term use.  
145 We assumed that at any given time, water table elevation is approximately equal to canal stage. We  
146 concede that at certain times this assumption might not hold e.g., immediately after or during storm

147 events; however, due to the high permeability of the aquifer and the daily time step used, the assumption  
148 holds for the majority of the time.

149 The goal of this study was to use DFA and modeling to investigate how the proposed raises in canal  
150 stage along C111 could impact soil and bedrock water contents in low lying farmlands located between  
151 canals C-111 and C-111E. The specific objectives were to: (1) apply DFA to identify the most important  
152 factors affecting temporal variation in soil and bedrock water contents, (2) develop a simplified DFA  
153 based regression model for predicting soil and bedrock water contents as a function of canal stage, and (3)  
154 use the developed simple regression model to predict the impact of proposed incremental raises in canal  
155 stage on soil and bedrock water contents at various elevations and distances from the canal.

## 156 **2. Materials and methods**

### 157 **2.1 Experimental site**

158 The study was conducted in southern Miami-Dade County, Homestead, Florida, United States in a  
159 small agricultural area approximately 17 km<sup>2</sup> (Fig. 1). The area is located east of ENP between SFWMD  
160 canals C111 and C111E which are planned to experience increases in canal stage under the C111 spreader  
161 canal project. Canal stage upstream in the two canals is controlled by a remotely operated spillway at  
162 S177 and a culvert at S178, respectively (Fig. 1). C111 is the larger of the two canals and the two join to  
163 become a single canal at the southern end of the study area which is managed using a gated spillway at  
164 S18C. It is proposed that stage will be increased by modifying operation of S18C and thus affect canal  
165 stage in the reach of C111 between S177 and S18C. The hydrogeological system at the study site consists  
166 of the Biscayne aquifer which is a highly permeable shallow unconfined aquifer with hydraulic  
167 conductivities reported to exceed 10,000 m/day, which explains the high connectivity between the canals  
168 and the aquifer (Chin, 1991). The shallow nature of the water table implies that evaporation from the  
169 groundwater could impact soil water content. The topography at this site is essentially flat with elevation  
170 ranging approximately between 1.2 to 2.0 m above sea level NGVD 29. The climate is subtropical with

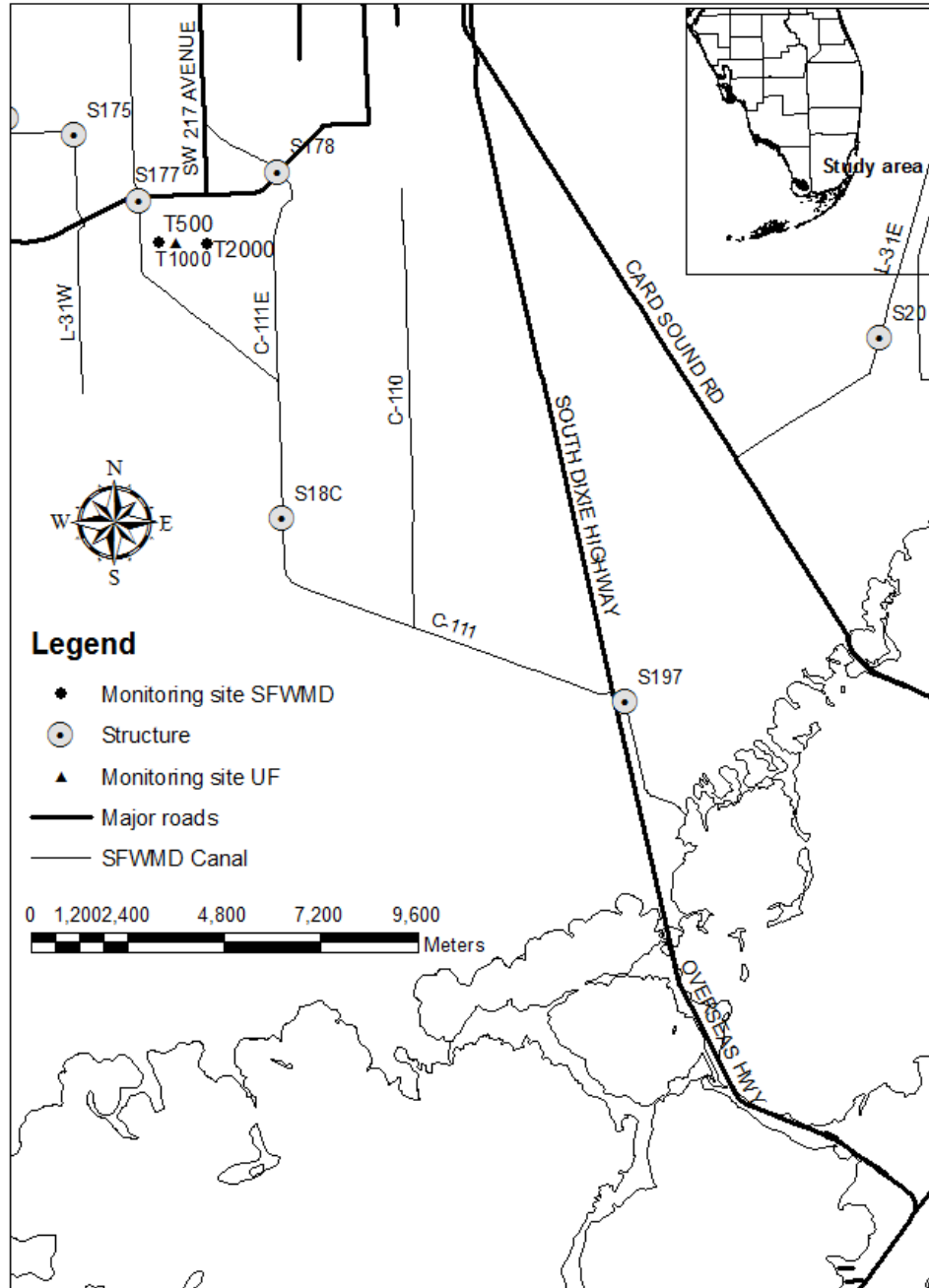


171 dry season (November to May), which is the growing season for vegetables, and wet season (June to  
172 October). Approximately two thirds of all the rain (average annual rainfall ranges between 1100 to 1524  
173 mm) is received during the wet season months.

174 The soil at the study site is very shallow (10 to 20 cm) with underlying limestone bedrock. According  
175 to Nobel et al. (1996), the soils east of C111 vary and could be classified as either Krome and Chekika  
176 very gravely loam (loamy skeletal, carbonatic, hyperthermic, Lithic Undorthents), or Biscayne Marl  
177 (loamy, carbonatic, hyperthermic) based on their physical characteristics. We performed particle size  
178 analysis using a standard 2-mm sieve and determined that the soils contain on average of 45% fine  
179 fractions and 55% gravel. Color analysis using the Munsell soil color charts (Munsell soil charts, 2000)  
180 and the color guide in Noble et al. (1996) identified the study site soils to be broadly characterized as  
181 Chekika soil series.

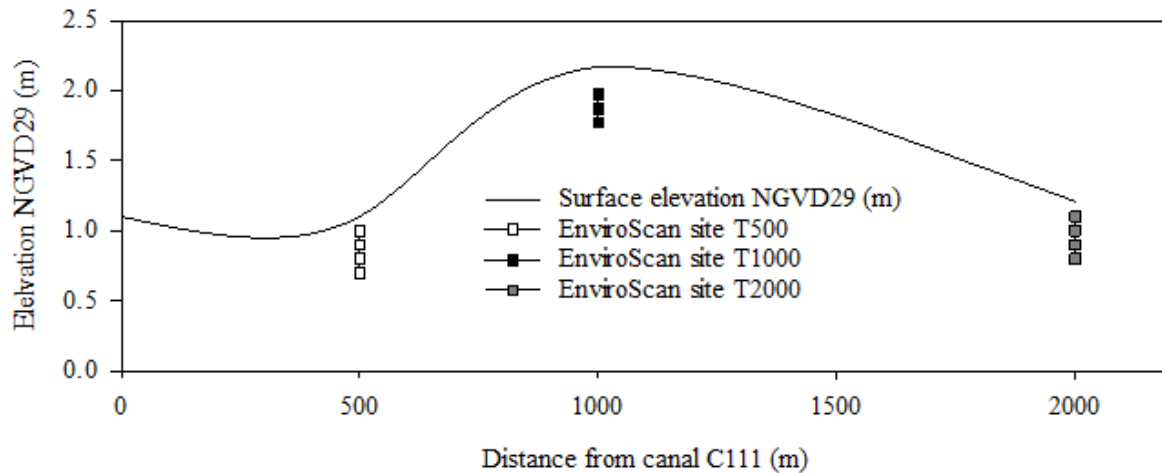
182 Three monitoring sites were used in this study located at 500, 1000 and 2000 m along a transect  
183 perpendicular to canal C111, the three sites also had varying topographies and represented areas expected  
184 to experience the greatest impact from the proposed raises in canal stage. Sites were selected to capture  
185 differences in soil texture within our study area; this was done with a soil survey map and site visits. Sites  
186 were also selected to ensure they were in privately owned agricultural low lying lands that were expected  
187 to be impacted by the rises in water table elevation. For each site: i) GPS coordinates and elevation data  
188 were collected, ii) groundwater wells were constructed and each was equipped with level loggers  
189 (Levelogger, Gold Solinst Canada Ltd., 35 Todd Rd, Georgetown, Ontario, Canada) to record water table  
190 elevation every 15 minutes, iii) multi-sensor capacitance probes (MSCP) (EnviroScan probes, Sentek  
191 Technologies, Ltd., Stepney, Australia) were installed at each site to monitor soil and bedrock water  
192 contents. Monitoring site locations are shown in Fig. 1; elevations are shown in Fig.2. Differences in the  
193 length of times series at the three sites was due to differences in the dates of installation of the EnviroScan  
194 probes (i.e., probes could only be installed when water was at least 50 cm below the ground surface) and

195 relocation of the probes due to initial poor installation. Site T500 was installed on August 25, 2010, while  
196 sites T1000 and T500 were installed on January 21, 2011.



197

198 Figure 1. . Map of the study area showing Everglades National Park, Taylor Slough, Florida Bay,  
199 SFWMD canal network and low lying agricultural areas east of canal C111 in south Florida



200

201 Figure 2. Showing a topographic changes along transect T and the elevation of the EnviroScan sensors at  
 202 the three sites.

## 203 2.2 Soil and bedrock water contents monitoring

204 Two EnviroScan probes were installed at each site for a total of six. Each access tube with a diameter  
 205 of 50.5 mm housed four sensors positioned at various elevations as shown in Fig. 2. The elevations  
 206 correspond to 10, 20, 30 and 40 cm from the ground surface at each site. The top 20 cm typically  
 207 represent the scarified soil layer which is used for crop production and the lower 20 cm represent the  
 208 underlying limestone bedrock in which plant roots cannot penetrate. To minimize the problem of air  
 209 pockets, we used fast setting cement slurry between the access tube and the soil. The purpose of installing  
 210 two EnviroScan probes at the same location was to ensure that at least one probe was functioning at any  
 211 given time. Due to the shallowness of the limestone bedrock at all the study sites, a motorized drill was  
 212 required to bore a hole that held the access tube in a vertical position. Water content data were logged  
 213 every 15 minutes and were downloaded weekly and averaged daily.

214 EnviroScans are an example of capacitance based sensors which measure frequency of an oscillating  
 215 electrical circuit. The oscillator is coupled electrically to capacitive elements that are made of two metal  
 216 cylindrical electrodes. The electrode system is arranged so the soil becomes part of the dielectric medium  
 217 affected by the fringing electromagnetic field. Volumetric soil water content affects the electrical

218 permittivity of the soil which in turn affects the capacitance causing the oscillation frequency to shift  
 219 (IAIA, 2008) since the soil dielectric constant is a combination of mineral particles (2-4), water (80), and  
 220 air (1). According to Dean et al. (1987) the oscillatory frequency from the capacitance soil water sensor  
 221 could be expressed eq. (1):

$$222 \quad F = \frac{1}{2\pi\sqrt{L}} \left( \frac{1}{C} + \frac{1}{C_b} + \frac{1}{C_c} \right)^{1/2} \quad (1)$$

223 Where  $C_b$  is the total base capacitance and  $C_c$  is the total collector capacitance and these represent  
 224 capacitances of internal circuit elements to which the electrodes are connected,  $L$  is the inductance of the  
 225 coil in the circuit, and  $C$  is the capacitance of the soil access tube system. Therefore capacitance of the  
 226 soil access tube system,  $C$ , can be expressed as a function of the soil dielectric constant ( $\epsilon$ ) and a value  $g$   
 227 representing the geometry of the sensor as shown in eq.(2).

$$228 \quad C = g \epsilon \quad (2)$$

229 Differences in oscillatory frequency among sensors at the same soil and bedrock water contents were  
 230 eliminated by normalizing the oscillatory frequency values using values of frequency when the sensor  
 231 was surrounded by water and air. The normalized oscillatory frequency is known as the scaled frequency  
 232 ( $SF$ ) and is estimated as in eq. 3. The manufacture default calibration equation (eq. 4) can be used to  
 233 convert scaled frequency to volumetric soil water content ( $\theta$ )

$$234 \quad SF = F - F_a / F_w - F_a \quad (3)$$

$$235 \quad \theta = (0.792 * SF - 0.0226)^{2.475} \quad (4)$$

236 where  $F$  is the oscillatory frequency value measured by the EnviroScan sensor,  $F_a$  is frequency value  
 237 when the EnviroScan probe is surrounded by air, and  $F_w$  is the frequency value when the EnviroScan  
 238 probe is surrounded by water. To avoid location specific calibration for each sensor, we use  $SF$  as

239 surrogate for  $\theta$  for investigating the effect of various factors on soil and bedrock water contents and thus  
240 did not use eq. (4). This approach was successfully applied by Ritter et al. (2009) when studying the  
241 effect of various factors on hydrologic fluxes in a forest top soil using refractive index from time-domain  
242 reflectometry (TDR) as a surrogate for volumetric soil water content. Gabriel et al. (2010) observed that  
243 the manufacturer's calibration equation overestimated volumetric soil water compared to the locally  
244 developed calibration equation. However, they noted that despite the overestimation of volumetric soil  
245 water content, the manufacturer's equation was able to reproduce temporal soil water dynamics.  
246 Therefore, if the goal is to measure relative changes in water content the manufacturer's default  
247 calibration equation is sufficient.

## 248 **2.3 Measurement and estimation of hydrologic variables**

249 Hydrologic variables including canal stage, water table elevation NGVD29 m, rainfall ( $P$ ), potential  
250 evapotranspiration ( $ET_o$ ) and groundwater evaporation ( $E$ ) were measured or estimated to assess their  
251 influence on soil and bedrock water content time series.

### 252 **2.3.1 Canal stage**

253 Canal stage data were measured at the S177 spillway for headwater (S177H) and tail water (S177T)  
254 every 15 minutes but daily averages were used. Canal stage data were measured by the SFWMD and are  
255 publically available from the online environmental database (DBhydro;  
256 [http://www.sfwmd.gov/dbhydroplsql/show\\_dbkey\\_info.main\\_menu](http://www.sfwmd.gov/dbhydroplsql/show_dbkey_info.main_menu)). During the first phase of the C111  
257 spreader canal project, the main operational adjustments will involve incrementally raising canal stage at  
258 S18C (Fig. 1) which will result in increased stage in the reach of C111 between the spillways at S177 and  
259 S18C.

### 260 **2.3.2 Water table elevation**

261 Water table elevation data were collected from three observation wells constructed at the three  
262 monitoring sites. Water table elevation was measured by the University of Florida (UF) every 15 minutes  
263 and averaged daily using a multi parameter pressure transducer at T1000 (Levelogger, Gold Solinst  
264 Canada Ltd., 35 Todd Rd, Georgetown, Ontario, Canada). Atmospheric corrections were included using a  
265 STS Barologger (Solinst Canada Ltd) in the well at T1000 (Fig. 1). Data were downloaded from the well  
266 weekly and as a quality control procedure, water table elevations were also measured manually with a  
267 Model 102 Laser water level well meter (Solinst, Canada Ltd). Wells T2000 (C111AE) and T500  
268 (C111AW) were installed and operated by the SFWMD and published on DBHydro.

### 269 **2.3.3 Rainfall**

270 Gauge adjusted Next Generation Radar (NEXRAD) rainfall data used in this study were obtained  
271 from the SFWMD. The United States National Weather Service operates two NEXRAD sites close to the  
272 study site (i.e., KBYX in Key West, FL and KAMX in Miami, FL) that provide 2 km x 2 km NEXRAD  
273 rainfall data. There are tradeoffs between rainfall estimated by rain gauges and NEXRAD. Rain gauges  
274 (e.g., tipping buckets) provide accurate point estimates of rainfall which are acceptable for frontal related  
275 rainfall events. However, in South Florida where most of the rainfall is received in summer and summer  
276 rainfall is dominated by conventional or tropical rainfall forming processes, rain gauges may fail to  
277 accurately represent the orientation of the rainfall front or fail to capture the entire rainfall event (Pathak,  
278 2008). On the other hand, measurement of rainfall by NEXRAD relies on the raindrop reflectivity which  
279 could be affected by factors such as raindrop size and microwave signal reflection by other particles in the  
280 atmosphere. Skinner et al. (2008) showed that the best of the two measurement methods is realized by  
281 using rain gauge or tipping bucket data to adjust NEXRAD values.

### 282 **2.3.4 Ground surface potential evapotranspiration**

283 Ground surface reference evapotranspiration ( $ET_0$ ) was computed from micrometeorological data  
284 (i.e., solar radiation, temperature, relative humidity and wind speed) obtained from a Florida Automated

285 Weather Network (FAWN; <http://fawn.ifas.ufl.edu/>) station located approximately 10 km northeast of the  
 286 study site at the Tropical Research and Education Center, Homestead, FL. The American Society of Civil  
 287 Engineers (ASCE) standardized Penman–Monteith equation was used to estimate  $ET_0$  values (ASCE,  
 288 2005). We assumed a crop with the following characteristics transpiring at a potential rate: crop height  
 289 (0.12 m), albedo (0.23), active leaf area index (1.44), and well illuminated leaf stomatal resistance (100.8  
 290 s/m). We applied the tool REF-ET (Allen, 2011) to calculate the ASCE standardized  $ET_0$  from weather  
 291 data.

### 292 2.3.5 Evaporation from the water table

293 Flux due to water table evaporation may influence soil and bedrock water contents. Previous studies  
 294 have shown that when canal influences are negligible, direct evaporation from the water table  
 295 significantly contributes to water table declines in the Biscayne aquifer (Merrit, 1996; Chin, 2008). Two  
 296 types of models are available to estimate evaporation from a water table: physically based models and  
 297 empirically based models. In this study, the latter was used because the former requires detailed data such  
 298 as coefficient of diffusion of water vapor through the soil and vapor pressure above the soil surface which  
 299 were not collected. Empirical models simply relate water table evaporation rate to the depth of the water  
 300 table below the ground surface and are used in groundwater studies (e.g., MODFLOW uses this approach;  
 301 Chin, 2008). We used a model similar to that proposed by McDonald and Harbaugh (1988) (eq. (5)). Chin  
 302 (2008) modified eq. (5) and obtained eq. (6) for south Florida conditions.

$$303 \quad \frac{E}{E_0} = \left(1 - \frac{d}{d_{cr}}\right), \quad d_{cr} = 100 * (170 + 8T), \quad d < d_{cr} \quad (5)$$

$$304 \quad \frac{E}{E_0} = \begin{cases} 1 & d \leq d_0 \\ 1 - \frac{d - d_0}{d_{cr}} & d_0 < d < d_{cr} \\ 0 & d \geq d_{cr} \end{cases} \quad (6)$$

305 where  $E$  is water table evaporation [mm/day],  $E_0$  (same as  $ET_0$ ) is the potential evaporation rate at the  
 306 ground surface [mm/day],  $d$  is the depth of the water table below the ground surface [m],  $d_{cr}$  is the critical  
 307 depth below which evaporation ceases [m],  $T$  is annual average air temperature [ $^{\circ}C$ ] which is  
 308 approximately  $25^{\circ}C$  in south Florida,  $d_0$  is water table depth above which water table evaporation  
 309 proceeds at potential rate i.e., at the rate similar to the ground surface evapotranspiration [m]. Chin (2008)  
 310 proposed parameters  $d_0$  and  $d_{cr}$  in eq. (6) at each observation well can be estimated from the least squares  
 311 best fit of eq. (7) and the parameters described as eq. (8) and (9).

$$312 \quad \frac{E}{E_0} = \alpha - \beta d \quad (7)$$

$$313 \quad d_0 = \frac{\alpha - 1}{\beta} \quad (8)$$

$$314 \quad d_{cr} = \frac{\alpha}{\beta} \quad (9)$$

#### 315 **2.4 Dynamic factor analysis**

316 DFA uses eq. (10) to describes a set of  $N$  observed time series (Lütkepohl, 1991; Zuur et al., 2003;  
 317 Ritter and Muñoz-Carpena, 2006). The goal in DFA is to keep  $M$  as small as possible while still obtaining  
 318 a good model fit. Including relevant explanatory variables helps to reduce some of the unexplained  
 319 variability in the observed time series.

$$320 \quad s_n(t) = \sum_{m=1}^M \gamma_{m,n} \alpha_m(t) + \mu_n + \sum_{k=1}^K \beta_{k,n} v_k(t) + \varepsilon_n(t) \quad (10)$$

$$321 \quad \alpha_m = \alpha_m(t-1) + \eta_m(t) \quad (11)$$



322 where  $s_n(t)$  is a vector containing the set of  $N$  time series being modeled (response variables),  $\alpha_m(t)$  is a  
 323 vector containing the common trends (same units as the response variables),  $\gamma_{m,n}$  are factor loadings or  
 324 weighting coefficients that indicate the importance of each of the common trends to each response  
 325 variable (unitless),  $\mu_n$  is a constant level parameter for shifting time series up or down,  $\nu_k(t)$  is a vector  
 326 containing explanatory variables, and  $\beta_{k,n}$  are weighting coefficients for the explanatory variables  
 327 (regression parameters) which indicate the relative importance of explanatory variables to each response  
 328 variable (inverse units to convert  $\nu_k(t)$  into response variable units), and  $\varepsilon_n(t)$  and  $\eta_m(t)$  are  
 329 independent, Gaussian distributed noise with zero mean and unknown diagonal covariance matrix. The  
 330 elements in the covariance matrix represent information that cannot be explained by the common trends  
 331 or the explanatory variables. The unknown parameters  $\gamma_{m,n}$  and  $\mu_n$  were estimated using the Expectation  
 332 Maximization (EM) algorithm that is described in Dempster et al. (1977) and Shumway and Stoffer  
 333 (1982). The common trends in eq. (11) were modeled as a random walk (Harvey, 1989) and were  
 334 predicted using the Kalman filter and EM algorithms. The regression parameters in eq. (10) are estimated  
 335 using the same procedure as used in linear regression (Zuur et al., 2003). DFA was implemented using a  
 336 statistical package called Brodgar Version 2.5.6 (Highland Statistics Ltd., Newburgh, UK).

337 The results from the DFA were interpreted in terms of the canonical correlations ( $\rho_{m,n}$ ), factor  
 338 loading ( $\gamma_{m,n}$ ), regression parameters ( $\beta_{k,n}$ ) and agreement between modeled and observed soil and  
 339 bedrock water contents (i.e., expressed as scaled frequency). The goodness-of-fit between modeled and  
 340 observed soil and bedrock water contents were quantified using the Nash-Sutcliffe coefficient of  
 341 efficiency ( $C_{eff}$ ; Nash and Sutcliffe, 1970), the Akaike's Information Criteria ( $AIC$ ; Akaike, 1974) and the  
 342 Bayesian information criterion ( $BIC$ ).  $C_{eff}$  provides an estimate of how well a model predicts an observed  
 343 data set, while  $AIC$  and  $BIC$  are relative measures of the goodness-of-fit of a statistical model. A model  
 344 with the  $C_{eff}$  closest to 1 and lowest  $AIC$  and  $BIC$  is the preferred DFA model. Cross correlations between

345 the soil and bedrock water content time series and common trends were measured using  $\rho_{m,n}$ . In our study  
 346  $\rho_{m,n}$  close to unity implied that the common trend was highly associated with water content time series.  
 347 Typically canonical correlations are classified as follows:  $|\rho_{m,n}| > 0.75$ , 0.5-0.75, and 0.3-0.5 as high,  
 348 moderate, and weak correlations, respectively. The influence of the explanatory variables on water  
 349 content time series were quantified using the magnitude of the  $\beta_{k,n}$  coefficients and their associated  
 350 standard errors which were used with a *t-test* to assess whether the response variable and explanatory  
 351 variables were significantly related.

352 DFA was implemented sequentially by varying the number of common trends  $M$  until a minimum  
 353  $AIC$  and  $BIC$  and  $C_{eff}$  closest to one were achieved (Zuur et al., 2003). After identifying the minimum  $M$ ,  
 354 different combinations of explanatory variables were introduced into the analysis until a combination of  
 355 common trends and explanatory variables that resulted in the most parsimonious model with best good-  
 356 of-fit indicators was achieved. The procedure followed here is similar to that described by Ritter et al.  
 357 (2009).

#### 358 **2.4.1 Explanatory variables**

359 Soil and bedrock water content time series are autocorrelated (Kaplan and Muñoz-Carpena, 2011)  
 360 while evapotranspiration and rainfall time series are not. For example, soil and bedrock water contents at  
 361 time  $t$  will depend on antecedent soil and bedrock water contents at time  $(t-1)$  whereas the rainfall today  
 362 does not depend on rainfall yesterday. Therefore in order to relate the soil and bedrock water content time  
 363 series and evapotranspiration and rainfall time series, we calculated a new variable called net cumulative  
 364 recharge ( $R_{net}$ ) using eq. 12.

$$365 \quad R_{net} = \sum_{t=1}^t P_t - \sum_{t=1}^t E_{o_t} \quad (12)$$

366 where  $P_t$  is the total rainfall for day  $t$  (mm) and  $E_{ot}$  is the potential evapotranspiration on day  $t$  (mm/day).  
367 Cumulative water table evaporation was also used instead of daily values. To minimize multi-collinearity  
368 of explanatory variables, we used mean water table elevation instead of water table elevation at each well.  
369 Before proceeding with the DFA, multi-collinearity of explanatory variables was quantified by computing  
370 variance inflation factors (VIFs) for each explanatory variable (Zuur et al., 2007).

## 371 **2.5 Simple predictive regression model for soil water content**

372 The simple regression model was developed from a DFA model having the minimum number of  
373 common trends required to explain underlying common patterns in the eleven time series and explanatory  
374 variables with significant influence on modeled soil water and bedrock water content time series. To  
375 enable practical use of the simple model, DFA was performed again for the identified model using non-  
376 normalized/non-standardized time series. After estimating the parameters through DFA the common  
377 trends were ignored in the model to derive a simple expression relating identified significant explanatory  
378 variables and soil and bedrock water contents. The period from August 25, 2010 to December 2011 was  
379 used to develop the regression model while the data from December 01, 2011 to June 30, 2012 was used  
380 to validate the new simple model. The developed simple model was then applied to predict the impact of  
381 a 6, 9 and 12 cm increase in canal stage on soil and bedrock water contents at the study sites.

## 382 **3. Results and discussion**

### 383 **3.1 Visual exploratory analysis of experimental time series**

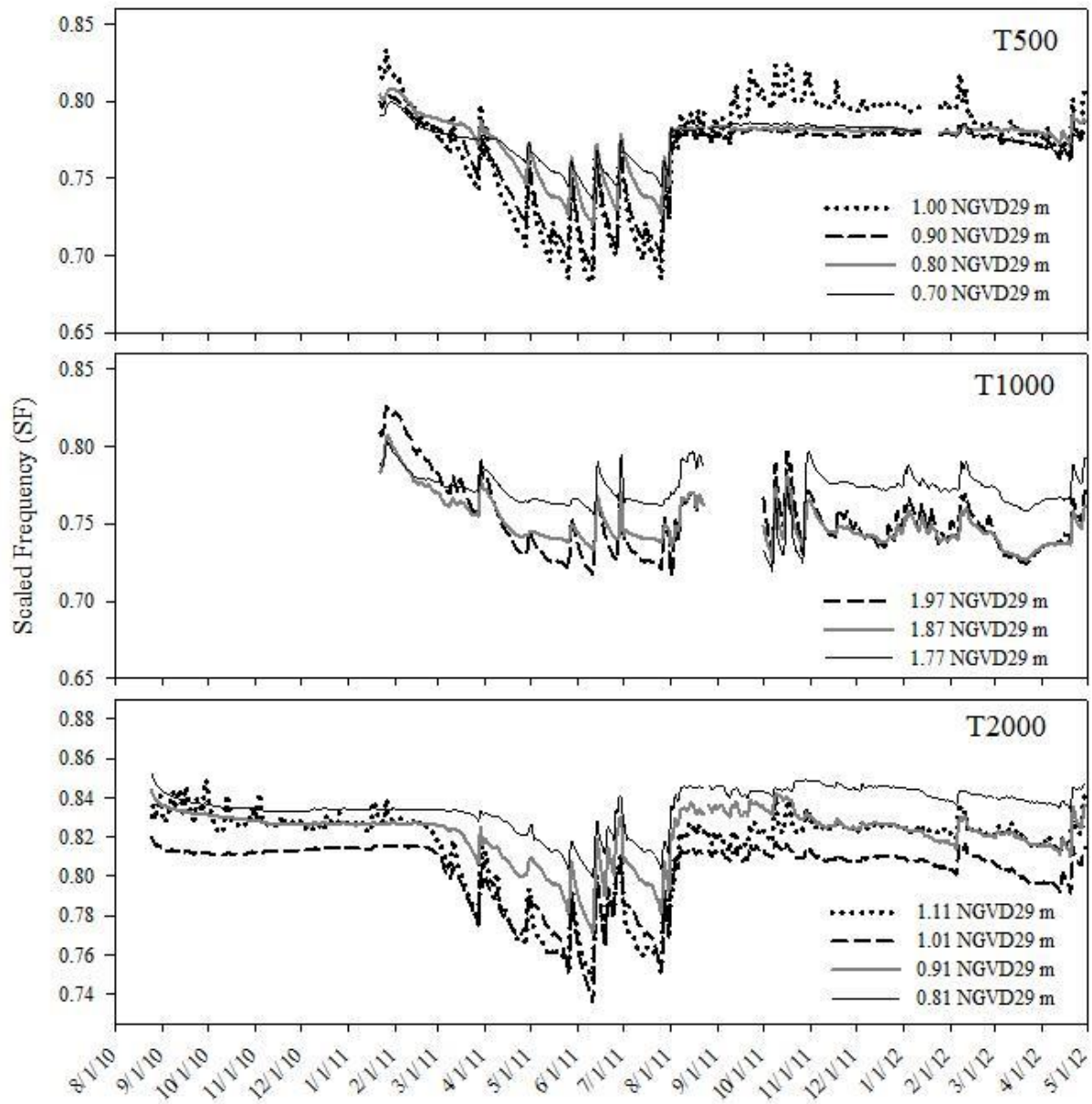
384 Visual inspection of soil and bedrock water content time series expressed as SF indicates that there  
385 were some common patterns in the temporal variation of soil and bedrock water contents at the three sites  
386 (T500, T1000 and T2000) along the transect perpendicular and east of canal C111. From February 2011  
387 to July 2011, soil and bedrock water contents gradually decreased at all monitoring elevations and all sites  
388 (Fig. 3). The gradual decrease in soil and bedrock water contents corresponded to the decline in canal  
389 stage and water table elevation (Fig. 4). The period from April to August was characterized by

390 pronounced drying and wetting cycles at all sites. The wetting or spikes in soil and bedrock water  
391 contents in this period correspond to the start of the rains while the drying cycles correspond to the  
392 increasing potential evapotranspiration during the same period (Fig. 4). The period from late March to  
393 July corresponds to the end of the growing season and beginning of the wet season. From August 2011 to  
394 February 2012, soil and bedrock water increased corresponding to stage operation criteria within the canal  
395 network that enhances water storage in the system.

396 However, there were observed differences in temporal soil and bedrock water variability at the three  
397 monitoring sites along the transect. Site T500 which is the shallowest and closest to the canal exhibited  
398 lack of temporal variation in bedrock water content at elevations less than 0.9 m NGVD29 while soil  
399 water content at 1.0 m NGVD29 exhibited temporal variation in the same period probably due to  
400 irrigation during the growing season. Site T1000 (i.e., approximately 1000 m from canal C111) exhibited  
401 the least increase in water content between March 2011 and June 2012. Unlike sites T500 and T2000, the  
402 trends in soil and bedrock water contents at T1000 were not identical to the temporal variation in canal  
403 stage or water table elevation suggesting micro-topography within the field might be affecting soil and  
404 bedrock water contents since this site had the highest elevation along the transect (Fig. 2). At site T2000  
405 (i.e., approximately 2000 m from canal C111), soil and bedrock water contents for the periods between  
406 August 2010 to March 2011 and August 2011 to February 2012 were similar characterized by small  
407 temporal variation similar to those exhibited at site T500. Sites T500 and T2000 have very similar  
408 elevation (1.1 and 1.2 m NGVD29 respectively) implying that topography or ground surface elevation  
409 might exert a stronger influence on temporal variation of soil and bedrock water contents compared to  
410 distance from the canal. Differences also existed at the different monitoring elevations with bedrock water  
411 content generally higher at the lowest elevation at each site. Other reasons for observed differences in  
412 water content at the different sites could be a combination of several factors such as differences in soil  
413 surface conditions, soil and limestone bedrock heterogeneity (specifically differences in soil water

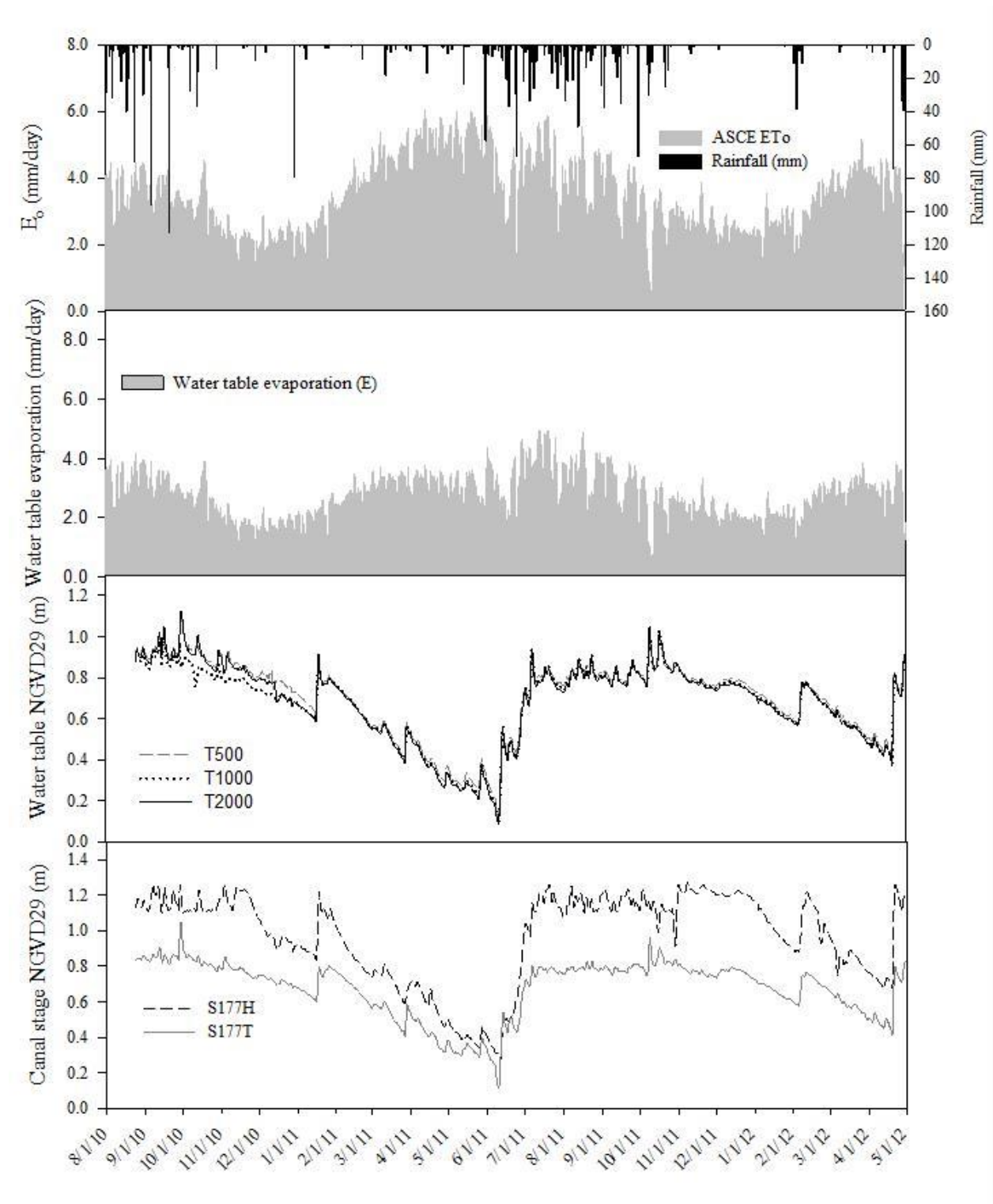
414 retention and unsaturated hydraulic conductivity) and differences in the environments surrounding the  
415 EnviroScan access tubes.

416 All the hydrologic variables monitored (Fig. 4) exhibited seasonal variations with rainfall increasing  
417 during wet season (May to October) resulting in increased water table elevation and canal stage.  $ET_o$  also  
418 increased during the wet season. In turn, decreased depth to water table and increased  $ET_o$  resulted in  
419 increased  $E$  (Fig. 4). The water table evaporation parameters for eq. (6) were computed following the  
420 procedure described by Chin (2009) in which steady declines in water table elevation particularly in the  
421 dry season when canal stage was maintained relatively constant are assumed to be caused by water table  
422 evaporation. Using data from a total of six wells (i.e., the 3 wells along transect T and 3 additional wells  
423 approximately 1 km north of the transect) within the vicinity of the study area, we obtained an average  
424 critical depth of 1.94 m which is within the range of 1.5 to 2.9 earlier reported by Chin (2009). We  
425 obtained a value of 0.59 m for the depth above which water table evaporation proceeds at the potential  
426 rate which is approximately half the average value of 1.4 reported by Chin (2009). The water table  
427 elevations at the three monitoring sites were very similar and also corresponded to the temporal variations  
428 in canal stage on the tail water side of the spillway at S177.



429

430 Figure 3. Temporal variation in scaled frequency (i.e., soil and bedrock water contents ) at three sites (i.e.,  
 431 T500, T1000 and T2000 with soil and bedrock water contents monitored at different elevations using  
 432 EnviroScan probes) along a transect perpendicular to C111 on the tail water side of the spillway at  
 433 structure S177 during the period August 2010 to June 2012.



434

435 Figure 4. Temporal variation in hydrologic factors evaluated for their influence on soil and bedrock water

436 contents at the study site during the period August 2010 to June 2012.

437 **3.2 Response and explanatory variables**

438 Visual inspection indicated that seasonality affects temporal variation of both response variables (i.e.,  
439 soil and bedrock water contents at different elevations) and explanatory variables (i.e.,  $ET_o$ , rainfall  $P$ ,  
440 water table elevation,  $E$  and canal stage). We attempted to remove seasonality effects through seasonal  
441 standardization following procedures described by Salas (1993), but this approach was abandoned since it  
442 resulted in poor model fit compared to the models in which seasonal effects were assumed to be masked  
443 in the common trends (i.e., average  $C_{eff} < 0.7$  and  $C_{eff} > 0.9$ , respectively). The poor model fit could be  
444 attributed to loss of information resulting from seasonal standardization. Ritter et al. (2009) also reported  
445 improved DFA model fit after back transforming refractive index data from a TDR as a surrogate for soil  
446 water content compared to seasonally standardized refractive index.

447 To facilitate interpretation of factor loadings and comparison of regression parameters as suggested  
448 by Zuur et al. (2004), all the time series were normalized. Therefore, the DFA results presented in  
449 reference to objective 1 are based on normalized time series data. Prior to performing the DFA,  
450 multicollinearity in explanatory variables was quantified by calculating Variance Inflation Factor (VIFs)  
451 for each explanatory variable. Threshold VIF of 5 was set as the highest, high values of VIF indicate  
452 multicollinearity in the explanatory variables which makes interpretation of regression results difficult  
453 (Ritter et al., 2009). As expected there was high multi-collinearity between water table elevation time  
454 series for different wells (VIFs  $> 30$ ), but this was considerably reduced when mean water table elevation  
455 at the three sites was used instead (i.e., VIFs  $< 2$ ). There was also high multi-collinearity between  
456 headwater and tail water canal stages at S177 (VIFs  $> 8$ ) implying that these two time series could not be  
457 used as explanatory variables in the same DFA model. Mean water table elevation was also correlated to  
458 canal stage S177 (VIFs  $> 10$ ) probably due to the high hydraulic connectivity between C111 and Biscayne  
459 aquifer. The correlation coefficient between canal stage and water table elevation time series was greater  
460 than 0.9.



461 **3.3 Common trends**

462 We developed the DFA model by exploring common trends and explanatory variables in relation to  
463 the 11 observed water content time series. Results of the DFA model selection are summarized in Table 1.  
464 We used the *AIC*, the *BIC* (which penalizes more strongly for over parameterization than the *AIC*) and the  
465  $C_{eff}$  statistic for deciding which of the DFA models with zero explanatory variables best described the  
466 response time series. Ten was the maximum number of common trends used to describe common  
467 variability in the 11 response water content time series. However, the goal of DFA is to minimize the  
468 number of common trends while maintaining a good model fit. Several models consisting of fewer  
469 numbers of common trends and noise were tested and model 4 with five common trends was determined  
470 to be the model with the minimum number of common trends required to describe the 11 response time  
471 series. Model 4 was selected since using  $M > 5$  resulted in negligible improvement in model goodness-of-  
472 fit measures while increasing the number of parameters to be interpreted. The three common trends with  
473 high ( $|\rho_{m,n}| > 0.75$ ) to moderate ( $0.5 < \rho_{m,n} < 0.75$ ) canonical correlations particularly at sites T500 and  
474 T2000 are shown in Fig. 5. Common trends 2 and 3 exhibited minor cross correlation with water content  
475 time series as measured by  $\rho_{m,n} < 0.5$  at all the sites and in the interest of brevity are not presented.

476 Visually, the unexplained variation in soil and bedrock water contents described by the common  
477 trends in Fig. 5 is similar to the seasonal variation of soil and bedrock water contents at sites T500, T1000  
478 and T2000 for the period August 2010 to August 2011. There was greater uncertainty as shown by a large  
479 (95%) confidence interval from August 25, 2010 to January 21, 2011 which is due to missing data for  
480 sites T500 and T1000 during this period. The first common trend exhibited high positive ( $|\rho_{1,n}| \geq 0.75$ )  
481 correlation with soil and bedrock water content time series at sites T500 and T2000 with low surface  
482 elevation (1.1 and 1.2 m NGVD29, respectively) compared to the moderate to weak correlation at site  
483 T1000 with ground surface elevation of 2.17 m NGVD29. Indicating that in addition to other factors, such

484 as irrigation during the growing season, micro-topography within the field influences temporal variations  
 485 in soil water content as it governs the effect exerted by the water table.

486 Table 1. Dynamic Factor Analysis (DFA) models tested based on the following goodness-of-fit measures:  
 487 AIC, BIC and  $C_{eff}$

Model	No. of common trends	Explanatory variables	No. of parameters	AIC <sup>1</sup>	BIC <sup>2</sup>	$C_{eff}$ <sup>3</sup>
<b>Step I (DFA model with K=0)</b>						
1	2	None	98	-2690.50	-2041.75	0.68
2	3	None	107	-4654.23	-3945.90	0.84
3	4	None	115	-5830.21	-5068.92	0.88
<b>4</b>	<b>5</b>	<b>None</b>	<b>122</b>	<b>-6901.47</b>	<b>-6093.84</b>	<b>0.97</b>
5	6	None	128	-7028.76	-6181.40	0.97
6	8	None	137	-7263.94	-6357.01	0.97
<b>Step II (DFA model with K&gt;0)</b>						
7	5	$R_{net}$ <sup>4</sup> ,	133	-7018.644	-6138.193	0.97
8	5	$R_{net}$ , $E$ <sup>5</sup>	144	-7797.525	-6844.255	0.98
9	5	S177T <sup>6</sup>	133	-7340.981	-6460.530	0.97
10	5	S177T, $R_{net}$	144	-7542.680	-6589.410	0.97
11	5	$R_{net}$ , $E$ , MWT <sup>7</sup>	155	-8052.436	-7026.346	0.98
12	5	MWT, $R_{net}$	144	-7444.030	-6490.761	0.97
<b>13</b>	<b>5</b>	<b><math>R_{net}</math>, <math>E</math>, S177T</b>	<b>155</b>	<b>-7922.346</b>	<b>-6896.257</b>	<b>0.98</b>

488 <sup>1</sup>AIC Akaike information criterion

489 <sup>2</sup>BIC Bayesian Information Criterion

490 <sup>3</sup> $C_{eff}$  Nash-Sutcliffe coefficient calculated based all the nine observed time series

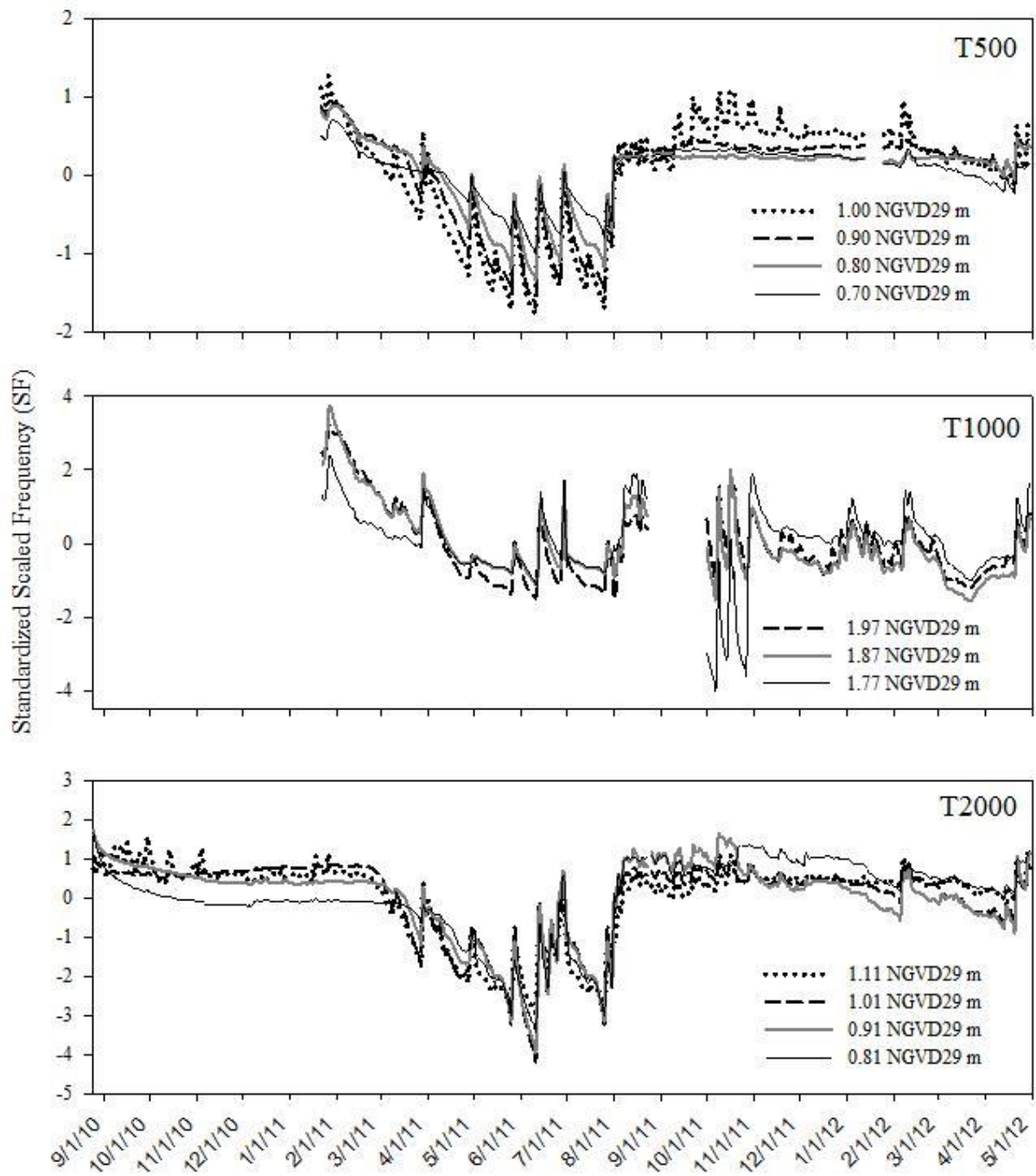
491 <sup>4</sup>Cumulative net surface recharge

492 <sup>5</sup> $R_{net}$  Cumulative water at table evaporation

493 <sup>6</sup>S177T Canal stage in C111

494 <sup>7</sup>MWT Mean water table evaporation

495



496

497 Figure 5. Common trends with 95% confidence interval describing unexplained temporal variation in  
498 scaled frequency as a surrogate for soil and bedrock water content and the canonical correlation for  
499 quantifying the correlation between water time series and the common trends, in the nomenclature for site

500 names the number represents distance from the canal in m, and the numbers in the parenthesis represent  
501 elevation NGVD 29 m.

### 502 **3.4 Relative contribution of explanatory variables**

503 Introducing net surface recharge, water table evaporation, and mean water table elevation or C111  
504 canal stage to model 4 resulted in the best models (11 and 13). Inclusion of explanatory variables in the  
505 DFA model also produced regression parameters ( $\beta_{k,n}$ ) and since response and explanatory variables  
506 were normalized, the regression parameters were used to quantify the relative influence of each  
507 explanatory variable on the modeled soil and bedrock water content time series. It is worth noting that  
508 substituting mean water table elevation in model 11 with canal stage as in model 13 resulted in *AIC* and  
509 *BIC* that were not substantially different and similar goodness-of-fit indicator (Table 1). Since part of the  
510 motivation for this research was to assess the effect of canal stage management on soil and bedrock water  
511 contents, further analysis was made on model 13 because canal stage data have a more consistent record  
512 compared to water table elevation data. At the study site, canal stage can be used as a good approximation  
513 to water table elevation due to the high permeability of the aquifer.

514 Model 13 fitted plots are shown in Figs. 6 to 8; these figures indicate that DFA modeling was  
515 successfully applied to describe temporal variations in soil and bedrock water contents at all three  
516 monitoring sites and elevations ( $C_{eff} > 0.9$ ). Results in Table 2 indicate that net surface recharge ( $R_{net}$ ) had  
517 a significant influence ( $t$  value  $> 2$ ) on the temporal variation of soil and bedrock water contents at sites  
518 T500, T1000, and T2000 but was not significant at lower elevations at sites T1000 and T2000 as shown ( $t$   
519 value  $< 2$ ). The significance of  $R_{net}$  could be attributed to rainfall ( $P$ ) patterns in the study area in which  
520 two thirds of the  $P$  was received in the wet season (SFWMD, 2011) and these large amounts of net water  
521 input to the vadose zone are sufficient to maintain soil and limestone bedrock near saturation, while  
522 absence of  $P$  in the dry season was responsible for the dry conditions. Lack of significance at lower

523 elevations at sites T1000 and T2000 could be attributed to heterogeneity in soils and bedrock (e.g.,  
524 differences in hydraulic conductivity), and differences in surface cover which influence  $ET_o$ .

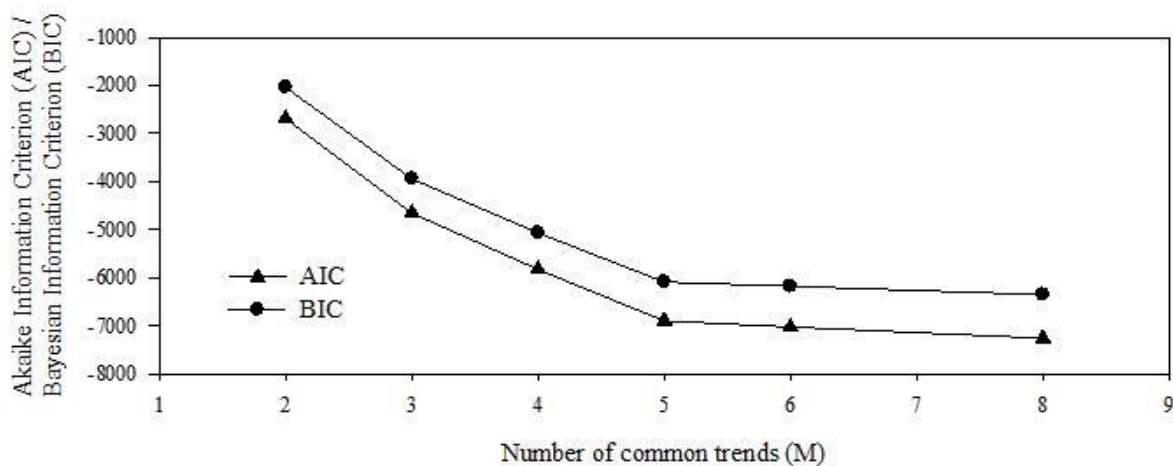
525 Water table evaporation was found to not significantly influence temporal variation of soil and  
526 bedrock water contents ( $t$  value  $<2$ ) at all the sites monitored. The non-significant effect of water table  
527 evaporation on soil and bedrock water content could be attributed to the fact that there is sufficient water  
528 for evaporation due to the shallow water table. However, the negative effect was stronger at site T1000,  
529 the negative effect is due to the fact that water table evaporation is a net loss from the vadose zone  
530 system. The small positive water table evaporation regression coefficient at T1000 and T2000 (Table 2)  
531 could be attributed to computational numerical errors. These results are worth highlighting given the fact  
532 that meteorological based methods for estimating  $ET_o$  like Penman Monteith equation are criticized for  
533 ignoring evaporation from the shallow water table meaning they might under estimate total  $ET_o$  losses.  
534 These observations could be attributed to that fact  $ET_o$  in such cases is not limited by water availability  
535 but by available energy only.

536 C111 canal stage on the tail water side at the S177 spillway (Fig. 1) had the strongest influence on  
537 soil and bedrock water content temporal variations ( $t$  value  $>7$ ) for most sites. This finding is significant  
538 because it confirms the hypotheses that the shallow water table and canal stage are highly connected and  
539 that canal stage can be used to predict soil water content at a given location. From a hydrologic  
540 perspective, these results were expected because in this case canal stage is used an approximation for the  
541 shallow water table which serves as the lower boundary condition for the vadose zone and therefore  
542 regulates available storage during the rainy season. Based on the relative magnitudes of the regression  
543 coefficients (Table 2), the overall contribution of canal stage on the respective soil and bedrock water  
544 content time series is higher than that of net recharge.

545 The factor loadings ( $\gamma_{1,n}$ ) for the five common trends are shown in Table 2, these represent the  
546 influence of each common trend on the modeled soil and bedrock water content time series at the

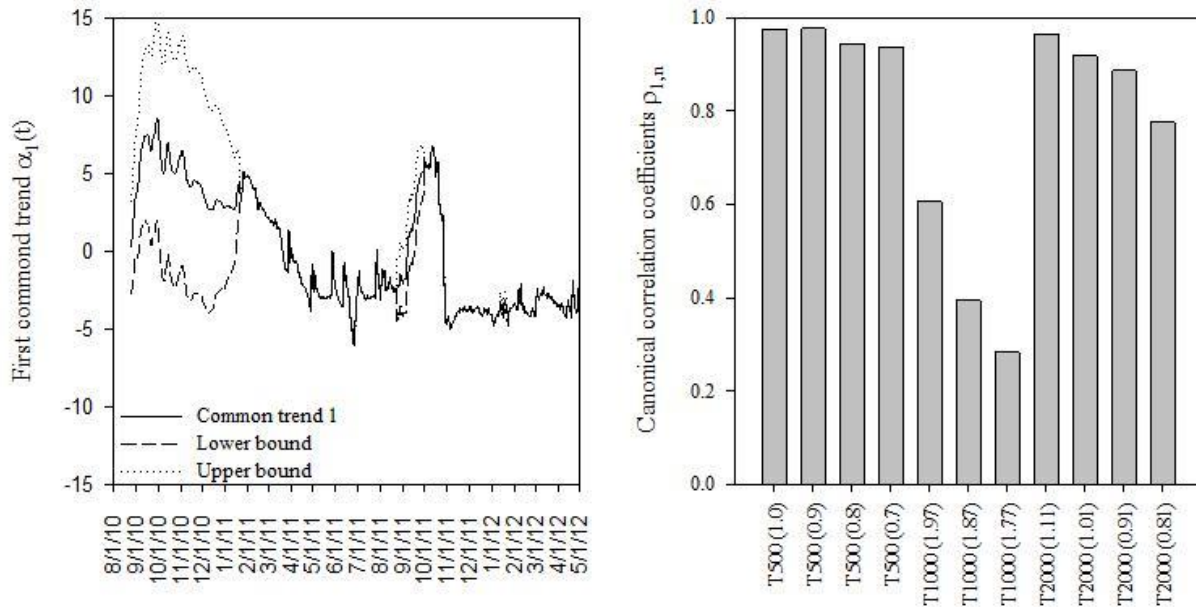
547 different monitoring sites and elevations. Since the time series in the DFA were normalized, the  
 548 coefficients  $\beta_{k,n}$  and  $\gamma_{1,n}$  can be compared (Zuur and Pierce, 2004). The results indicate that trend 1 was  
 549 very critical for describing unexplained variation in soil water dynamics at site T2000, while common  
 550 trends 2 and to a lesser extent 3 were more critical for describing unexplained variation in soil water  
 551 content at site T1000. Site T500 was sufficiently described by the explanatory variables and constant level  
 552 parameters given their magnitudes were larger compared to the  $\gamma_{1,n}$ . Trends 4 and 5 had minor effects at  
 553 all the monitoring sites.

554 Overall at all the sites, compared to regression coefficients and the constant level parameters,  
 555 common trends had less influence on soil and bedrock water dynamics. However, since the values of the  
 556 factor loadings are not zero (i.e., they account for some unexplained variability) especially at T2000 and  
 557 site T1000, this implies that the information provided by the hydrologic variables used as the explanatory  
 558 variables in the DFA models only account for part of the unexplained variability in the temporal variation  
 559 of the soil and bedrock water contents. Other information such as irrigation, differences in soil surface  
 560 conditions, differences in the environment surrounding the EnviroScan access tube, and variation in soil  
 561 hydraulic properties not considered in this study might account for part of the remaining unexplained  
 562 variability.

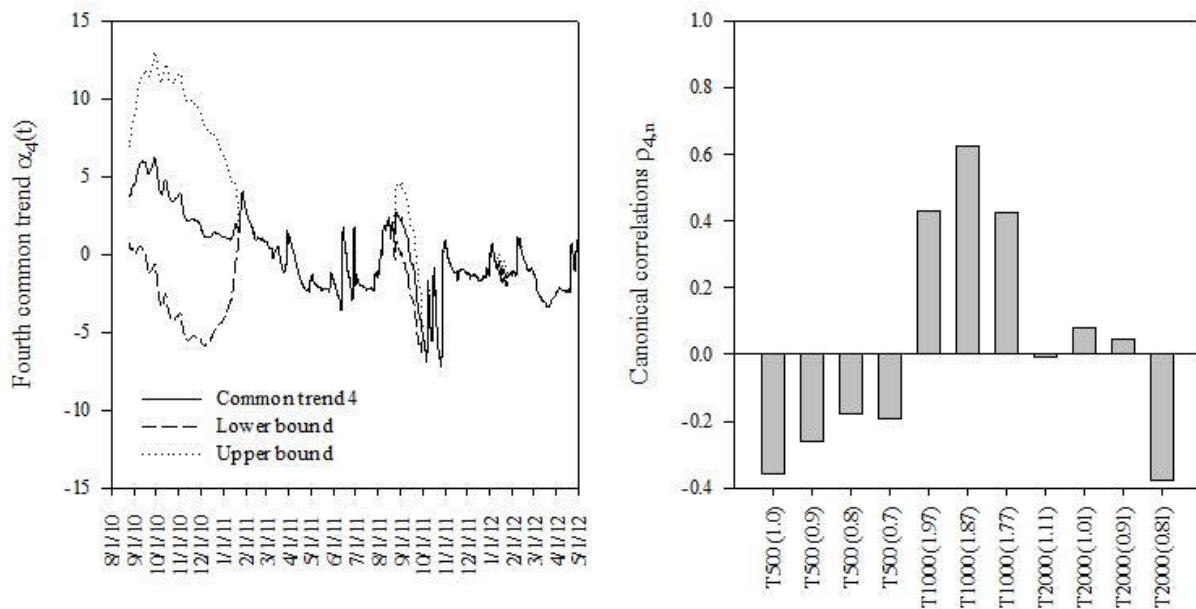


563

564 Figure 6. Fitted Dynamic Factor Model (DFM) and observed temporal variation in scaled frequency (used  
 565 as a surrogate for soil and rock water) in gravely loam soils and limestone bedrock at a site located 500 m  
 566 along a transect from C111 and the numbers in the parentheses indicate elevations.



567  
 568 Figure 7. Fitted Dynamic Factor Model (DFM) and observed temporal variation in scaled frequency  
 569 (used as a surrogate for soil and rock water) in gravely loam soils and limestone bedrock at a site located  
 570 1000 m along a transect from C111 and the numbers in the parentheses indicate elevations.



571  
 572 Figure 8. Fitted Dynamic Factor Model (DFM) and observed temporal variation in scaled frequency  
 573 (used as a surrogate for soil and rock water) in gravely loam soils and limestone bedrock at a site located  
 574 2000 m along a transect from C111 and the numbers in the parentheses indicate elevations.

575 Table 2. Dynamic Factor Analysis results for model 13 with 5 common trends and 3 explanatory  
 576 variables

$s_n$	$\gamma_{1,n}$	$\gamma_{2,n}$	$\gamma_{3,n}$	$\gamma_{4,n}$	$\gamma_{5,n}$	$\mu_n$	$\beta_{Rnet}$	$\beta_E$	$\beta_{C111stage}$	$C_{eff}$
<sup>1</sup> T500 (1.0)	0.05	0.02	0.04	-0.02	-0.03	0.28 (0.6)	0.34 (6.9)	0.00 (0.0)	0.24 (8.8)	0.93
T500 (0.9)	0.05	0.06	0.03	-0.04	-0.05	0.37 (0.5)	0.24 (3.5)	-0.14 (-0.3)	0.29 (8.3)	0.94
T500 (0.8)	0.04	0.06	0.03	-0.03	-0.04	0.34 (0.6)	0.20 (3.2)	-0.17 (-0.5)	0.22 (7.5)	0.90
T500 (0.7)	0.03	0.02	0.01	0.00	-0.01	0.13 (0.6)	0.18 (7.1)	-0.09 (-0.7)	0.13 (9.1)	0.90
T1000 (1.97)	0.04	0.16	0.13	-0.02	0.00	0.95 (0.9)	0.47 (3.1)	-0.53 (-0.7)	0.62 (8.7)	0.85
T1000 (1.87)	0.04	0.20	0.11	0.01	0.01	0.82 (0.8)	0.38 (2.1)	-0.61 (-0.8)	0.70 (8.5)	0.81
T1000 (1.77)	0.01	0.50	0.01	0.00	0.00	0.00 (0.0)	0.44 (1.1)	0.23 (0.1)	0.77 (4.6)	0.67
T2000 (1.11)	0.10	0.04	0.06	-0.07	0.01	0.07 (0.1)	0.13 (2.0)	0.05 (0.1)	0.50 (11.6)	0.99
T2000	0.13	0.05	0.06	-0.02	0.06	-0.09 (-0.1)	0.03 (0.3)	-0.03 (0.0)	0.68 (13.2)	0.90



---

(1.01)											
T2000											
(0.91)	0.17	0.03	0.06	0.01	-0.01	-0.12 (-0.1)	0.05 (0.4)	-0.22 (-0.3)	0.71 (12.4)	0.93	
T2000											
(0.81)	0.16	0.04	-0.03	-0.02	-0.02	-0.31 (-0.3)	0.08 (0.8)	0.02 (0.0)	0.46 (8.8)	0.96	

---

577  $\gamma$  Factor loading corresponding to common trend 1 to 5 and observation,  $n= 1, 2, 3, \dots, 11$

578  $\mu$  Constant level parameter in dynamic factor model with associated  $t$ -value in parenthesis

579  $\beta$  Regression parameter corresponding to the 3 explanatory variables (net recharge [ $R_{net}$ ], water table evaporation [E], and canal stage in C111 [C111stage]) with associated  $t$ -value in parenthesis

581  $C_{eff}$  is Nash-Sutcliffe coefficient

582 <sup>1</sup>Site name nomenclature; T refers to transect name T, number refers to distance from canal and number in parentheses refers to elevation NGVD29 m

584  $n$  number of observations

### 585 **3.5 Predicting soil and bedrock water contents using a simplified dynamic factor analysis based** 586 **model**

587 To enable practical application of the DFA model, the common trends and two of the exploratory  
588 variables included in model 13 were used in a new DFA model with non-standardized time series. This  
589 new model was referred to as model 14. To further simplify model 14, we ignored the common trends to  
590 derive a simple model that predicts soil and bedrock water contents as function of net recharge and canal  
591 stage expressed as eq. 13

$$592 \quad SF(X, Z, t) = \beta_{R_{net}}(X, Z) R_{net}(t) + \beta_{C111}(X, Z) S177T(t) + \mu(X, Z) \quad (13)$$

593 where  $SF(X, Z, t)$  is the SF at distance  $X$  from the canal, at elevation  $Z$ , and time  $t$ , other terms in  
594 are previously described and varies with elevation and distance from the canal. The coefficients  
595 for eq. 13 at all the sites and monitoring elevations are obtained from Table 3. The  $C_{eff}$  in Table 3 are  
596 calculated based on eq. 13 with common trends removed. As expected, performance of the simple model  
597 (eq. 13) was lower as shown by the reduction in  $C_{eff}$  (Table 3 and Figs. 9 to 10) compared to the DFA  
598 models that include common trends particularly for site T1000.

599 Since factor loadings are not zero for all the trends (Table 3), this suggests that the explanatory  
600 variables (net recharge and canal stage) used in the DFA model are not sufficient to explain all the  
601 observed variations in the soil and bedrock water content time series. This is particularly true at site

602 T1000 which is affected by 4 out of the 5 common trends. Common trend number 2 appears to affect all  
 603 the sites, it probably masks common variation such seasonal changes in rainfall, evapotranspiration and  
 604 canal stage. Other common trends had minor effects at sites at all the other sites particularly at site T1000.  
 605 The difference in response at site T1000 could be attributed to differences in elevation as shown in Fig. 2,  
 606 site T1000 has a higher surface elevation and hence larger depth to water table.

607 The results in Table 3 also underscore the point that the effect of canal stage is stronger at low  
 608 elevation sites T500 and T2000 compared to T1000. Thus, proper interpretation of modeling results in  
 609 this area requires accurate quantification of micro-topography. Model performance ranged from good at  
 610 sites T500 and T2000 to poor at site T1000 with root mean square error (RMSE) ranging from 0.005 to  
 611 0.01. Figs. 9 to 10 show model performance during the calibration and validation periods, after removing  
 612 the common trends, it can be seen that the simple model misses the peaks but is able to generally predict  
 613 the temporal variation in soil and rock water content. The simple model (eq. 13) could be improved by  
 614 using location specific water table elevation since canal stage is simply a good approximation of the mean  
 615 water table elevation. Another simple sigmoidal regression model to predict soil and bedrock water  
 616 contents from canal stage proposed by Kaplan et al. (2010a) was tried but later abandoned due to lower  
 617  $C_{eff}$  (i.e., averaging 0.2). This approach is based on the physical concept of drain to equilibrium. However,  
 618 for our study site this condition was hard to achieve since during the dry season irrigation was taking  
 619 place and in the rainy season there was frequent rainfall hence by removing data points corresponding to  
 620 rainfall or irrigation, very few data points were left to develop a useful sigmoidal model for predicting soil  
 621 and bedrock water content from canal stage.

622 Table 3. Dynamic Factor Analysis results for model 14 with 5 common trends and 2 explanatory  
 623 variables implemented with non-standardized time series

$S_n$	$\gamma_{1,n}$	$\gamma_{2,n}$	$\gamma_{3,n}$	$\gamma_{4,n}$	$\gamma_{5,n}$	$\mu_n$	$\beta_{Rnet}$	$\beta_{c11stage}$	$C_{eff}$	$C_{eff}$
<sup>1</sup> T500 (1.0)	-0.003	0.000	0.000	0.000	0.000	0.72	0.14	0.06	0.73	0.70
T500 (0.9)	-0.001	-0.004	0.000	0.000	0.000	0.72	0.11	0.04	0.61	0.62

T500 (0.8)	-0.001	-0.004	0.000	0.000	0.000	0.75	0.09	0.02	0.51	0.56
T500 (0.7)	-0.001	-0.002	0.002	0.000	0.000	0.76	0.07	0.01	0.81	0.74
T1000 (1.97)	0.003	-0.005	-0.002	0.000	0.001	0.73	0.10	0.02	0.61	0.15
T1000 (1.87)	0.002	-0.003	-0.001	0.000	0.001	0.74	0.05	0.01	0.51	0.13
T1000 (1.77)	0.001	-0.003	0.001	-0.002	0.000	0.77	0.02	0.00	0.25	0.11
T2000 (1.11)	0.000	-0.003	-0.002	0.000	0.000	0.76	0.08	0.06	0.70	0.61
T2000 (1.01)	0.000	-0.003	0.000	0.000	0.001	0.76	0.05	0.05	0.60	0.67
T2000 (0.91)	0.000	-0.002	0.000	0.000	0.001	0.77	0.03	0.04	0.67	0.63
T2000 (0.81)	-0.001	-0.001	0.000	0.000	0.001	0.80	0.02	0.02	0.65	0.61

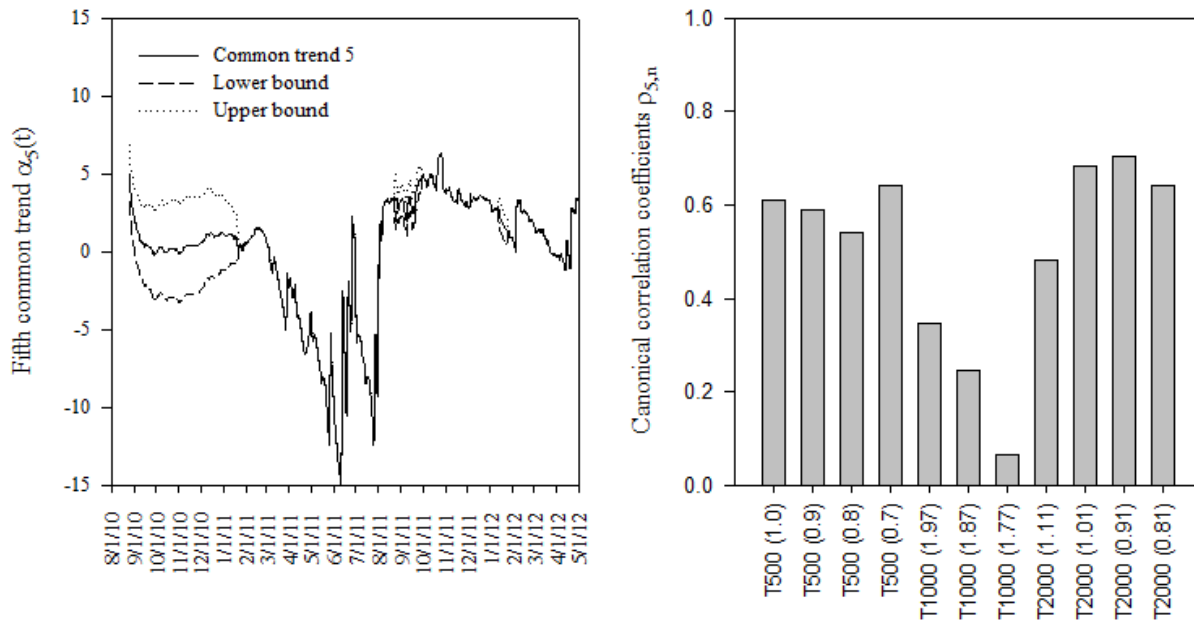
624  $\gamma$  Factor loading in the dynamic factor model

625  $\mu$  Constant level parameter in dynamic factor model

626  $\beta$  Regression parameter corresponding to the 2 explanatory variables (net recharge [ $R_{net}$ ], and canal stage in C111 [C111stage])

628 <sup>1</sup>Nash-Sutcliffe coefficient are calculated after ignoring common trends

629 <sup>2</sup>Nash-Sutcliffe coefficient during validation

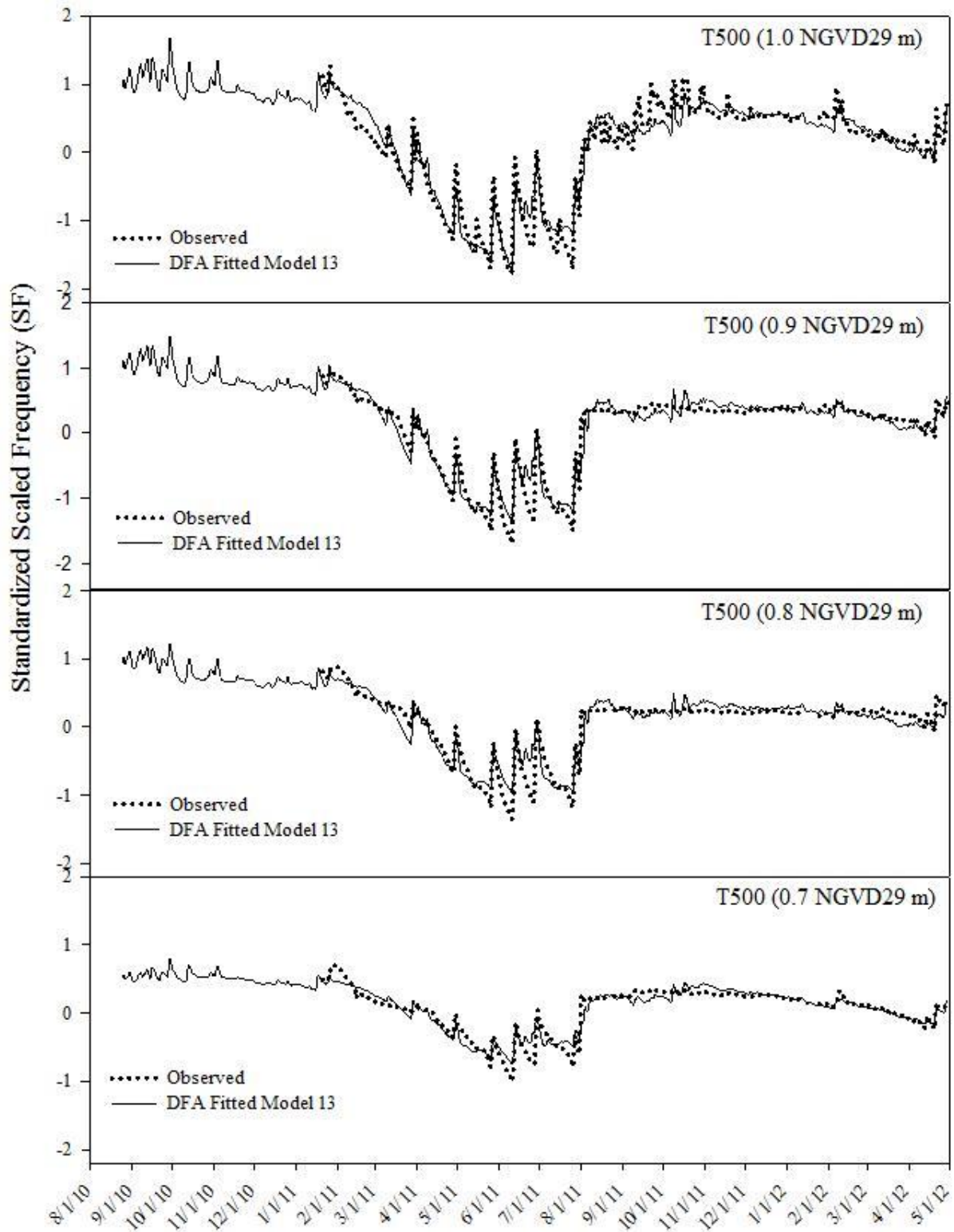


630

631 Figure 9. Performance of a simple model for predicting scaled frequency (used as a surrogate for soil and

632 bedrock water content) as a function of canal stage and net recharge at specific elevations in parentheses

633 NGVD29 at a site located 500 m along transect T from C111.



635 Figure 10. Performance of a simple model for predicting scaled frequency (used as a surrogate for soil  
636 and bedrock water content) as a function of canal stage and net recharge at specific elevations in  
637 parentheses NGVD29 at a site located 2000 m along transect T from C111.

### 638 **3.6 Assessing the impact of proposed operational changes in C111 canal stage management on soil** 639 **and bedrock water contents**

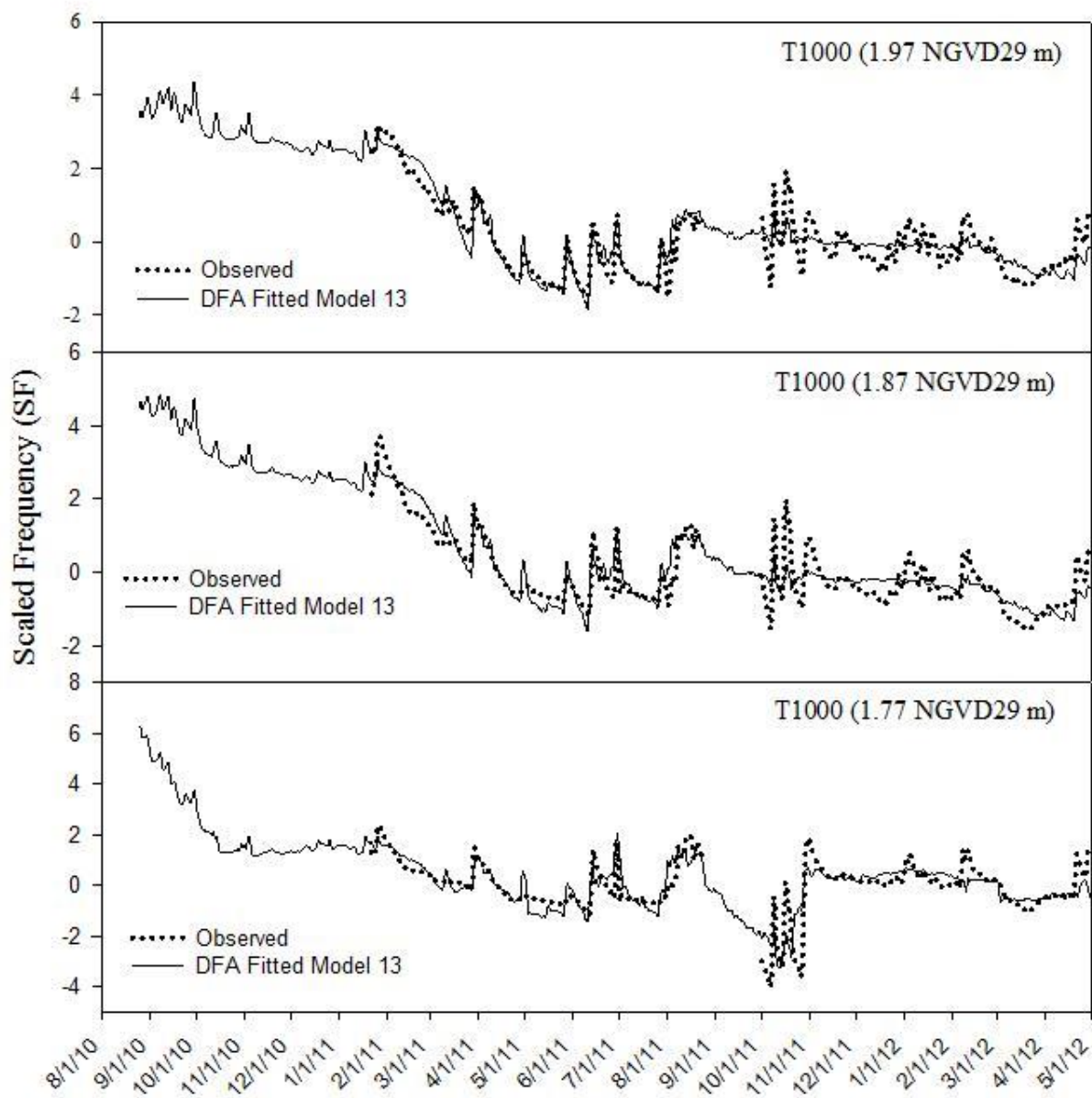
640 The low lying agricultural areas east of canal C111 are anticipated to experience the greatest  
641 impact from the proposed changes in C111 stage operation (i.e., canal stage increases of 6, 9, and  
642 12 cm); a simple DFA based regression model eq. 13 was proposed to predict the soil and  
643 bedrock water contents as a function of canal stage. We considered the period from January 01,  
644 2012, to June 30, 2012 for the analysis. Increases in canal stage were computed by simply adding  
645 the proposed incremental rises in canal stage to the daily canal stage recorded at S177T while  $P$   
646 and  $ET_o$  from the original dataset were not changed.

647 The results from using this simplified DFA based model (Figs. 11 and 12) indicate that the  
648 proposed increases in canal stage were predicted to have changes in daily mean SF for the study  
649 period (i.e., which is used as a surrogate for soil and bedrock water contents) of <1% at all sites  
650 and all elevations monitored. The range in daily SF differences was 0.065 to -0.024 and 0.075 to  
651 -0.041 at sites T500 and T2000 respectively, which indicates that the simple model over  
652 predicted and under predicted SF on certain days during the study period. However, note that the  
653 daily differences in SF are not substantially large, this may be attributed to already high values of  
654 soil and bedrock water contents observed in the area. On an event basis the potential to flood or  
655 saturate the root zone would depend on the size of the storm and storm contingency planning for  
656 lowering of canal stage in anticipation of heavy storms. Since we showed using DFA that soil  
657 and bedrock water contents were significantly affected by canal stage and net recharge.

658 The simple model used in this evaluation was more accurate at sites T500 and T2000 and  
659 therefore results at these two sites would be considered with less uncertainty. Soil and bedrock  
660 water responses to incremental raises in canal stage were not computed for site T1000 since  
661 results at this site would be considered less accurate (greater uncertainty) because model  
662 performance was very poor at this site. Figs. 11 and 12 show that changes in soil and bedrock  
663 water contents were more noticeable at the highest elevation. However, at the lowest elevations  
664 monitored the difference between mean SF before and after all increments was zero at T500.  
665 These observations could be attributed to the fact that low elevation sites are normally close to  
666 saturation. For example, at site T500 (0.7) when water elevation was above the sensor (implying  
667 saturated conditions), SF was recorded as 0.786 compared to average SF of 0.775 for the study  
668 period meaning small changes in water table may not result in substantial changes in soil water  
669 content since the pores are already near saturation.

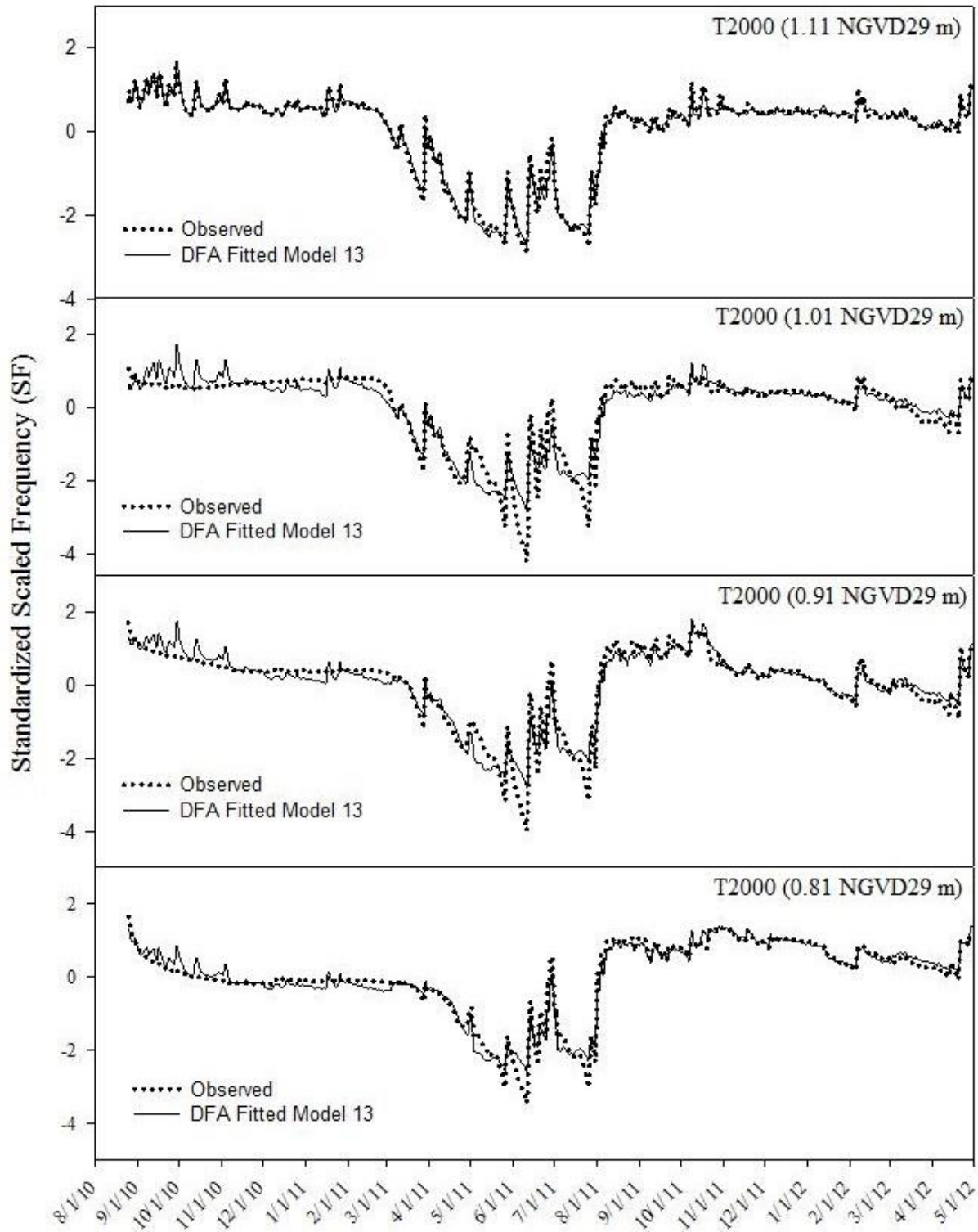
670 It is worth noting that the simple model developed above should be applied with the  
671 following limitations in mind. The model does not account for water input from irrigation and  
672 therefore would under predict soil and bedrock water content during the growing season, the  
673 model also uses canal stage as an approximation for water table elevation at a specific location  
674 although the two are usually close there may be deviations especially after large rainfall events, it  
675 ignores water content drivers that were masked in the common trends, and lastly the simple  
676 model ignores the effect of  $E$  which might vary based on micro-topography within the field as  
677 well as differences in land surface cover conditions. Finally, although the simplified DFA based  
678 model is empirical in nature, the results suggest it can be used as a preliminary tool to relate the  
679 potential impacts of surface water management decisions on soil and bedrock water contents in  
680 low lying farmlands adjacent to canal C111. This is because during the duration of the study, we

681 able to capture a wide range of variation in canal stage and water table elevation e.g., on June 10,  
682 2011 we recorded canal stage and groundwater table elevation of 0.14 m NGV29 which is lower  
683 than the optimum design stage of 0.6 m for the reach of C111 between S 18C and S177 under  
684 current canal stage operational criteria. During the summer of 2011 (on October 09, 2011) we  
685 recorded canal stage and groundwater levels as high as 0.9 and 1.02 m NGVD29 which is close  
686 to the level supposed to trigger the spillway to open at S177 under current operational criteria.



687

688 Figure 11. Boxplots showing soil and rock water content as measured using scaled frequency at site T500  
689 before and after 6, 9 and 12 cm increase canal at structure S18C along C111.



690



691 Figure 12. Boxplots showing soil and rock water content as measured using scaled frequency at site  
692 T2000 before and after 6, 9 and 12 cm increase canal at structure S18C along C111.

693

694 **4.0 Summary and Conclusions**

695 The response of soil and bedrock water contents to incremental raises in canal stage proposed under  
696 the C111 spreader canal project whose goal is to restore the hydrology of ENP while maintaining flood  
697 protection in the adjacent agricultural areas was investigated using DFA. The study objectives were to use  
698 DFA to identify the important factors driving temporal variation in soil and bedrock water content above  
699 the shallow water table at the study site, develop a simple model for predicting soil water content as a  
700 function of canal stage and assess the effect of the proposed incremental raises in canal stage on soil and  
701 bedrock water contents. Five was the minimum number of common trends required to account for the  
702 unexplained variation in the eleven observed soil and bedrock water content time series while producing  
703 an acceptable model fit. Introduction of explanatory variables i.e., net recharge, water table evaporation,  
704 and canal stage or water table elevation to the DFA model resulted in lowering AIC and BIC values while  
705  $C_{\text{eff}}$  values did not substantially change. Evaluation of the regression coefficients indicated that net  
706 recharge and canal stage had significant effects on temporal variation of soil and bedrock water contents  
707 while the effect of water table evaporation was non-significant. Based on the magnitude of the regression  
708 coefficients, canal stage had the greatest influence on the temporal variation of soil and bedrock water  
709 contents at all elevations and distances from the canal at the locations monitored. The effect of canal stage  
710 and mean water table elevation in the DFA model was similar confirming the high hydraulic connectivity  
711 between the canal and Biscayne aquifer.

712 Based on the high connectivity between surface water in the canal and Biscayne aquifer, a simple  
713 DFA based regression model (DFA model in which the common trends were removed), was developed to  
714 predict soil and bedrock water contents as a function of canal stage and net recharge at various elevations.  
715 The performance of the simplified regression model was described as good to acceptable at sites with low  
716 elevation (i.e., water table elevation within 1m from the ground surface) and poor at the location at with  
717 water table depth greater than 1.5 m. These findings highlight the effect of micro-topography within the  
718 field on soil water content. The study also revealed that factor loadings were not zero for all the common

719 trends suggesting that the explanatory variables (net recharge and canal stage) used in the DFA model are  
720 not sufficient to explain all the observed variations in the soil and bedrock water content time series.

721 The effect of the proposed 3 incremental raises in canal stage on soil and bedrock water content was  
722 simulated using the developed simple DFA based regression model for a total of 181 days beginning  
723 January 01, 2012. The results based on the data collected indicate that the proposed raises in canal stage  
724 would result in negligible changes in average soil and bedrock water contents at low elevations monitored  
725 in this study based. Changes in soil water content near the ground surface were more noticeable. The  
726 DFA based regression model developed is limited in its prediction ability to the range of canal elevations  
727 and net recharge by which it was developed. The uncertainty in predictions could be minimized by  
728 continuously updating the regression coefficients and constant level parameters as more data on response  
729 and explanatory variables are collected. The results of the regression model could be further evaluated  
730 using physically based modeling approaches. The approach used in this study could be applied to any  
731 system in which detailed physical modeling would be limited by inadequate information on parameters or  
732 processes governing the physical system.

### 733 **Acknowledgements**

734 The authors would like to thank the South Florida Water Management District for providing the funding  
735 for this study, the University of Florida IFAS Tropical Research and Education Center, and the University  
736 of Florida Agricultural and Biological Engineering Department, Mr. Vito Strano and Mr. Sam Accursio  
737 for allowing us to use their lands and Mrs. Tina Dispenza for her contribution towards data collection and  
738 processing. We also like to thank the three anonymous reviewers whose comments and suggestions  
739 greatly improved this manuscript.

740

741 **References**

- 742 Akaike, H., 1974. A new look at the statistical model identification. *IEEE Trans. Automat. Control* 19,  
743 716–723.
- 744 ASCE, 2005., The ASCE Standardized Reference evapotranspiration Equation. Task Committee on  
745 Standardization of Calculation of Reference ET. Environment and Water Resources Institute of  
746 ASCE. 200 p.
- 747 Allen, R., 2011. REF-ET: Reference Evapotranspiration Calculation Software. User Manual.
- 748 Barquin, L.P., Migliaccio, K.W., Muñoz-Carpena, R., Schaffer, B., Crane, J.H., Li, Y.C., 2011. Shallow  
749 Water Table Contribution to Soil-Water Retention in Capillary Fringe of a Very Gravelly Loam  
750 Soil of South Florida. *Vadose Zone J*, 10:1–8.
- 751 Chin, D., 1991. Leakage of clogged channels that partially penetrate surficial aquifers. *ASCE J. Hydraulic*  
752 *Engineering*. 117, 467-488.
- 753 Chin, D., 2008. Phenomenological models of hydrologic processes in south Florida. *J. Hydrol.* 349, 230–  
754 243.
- 755 Dean, T.J., Bell J.P. Baty A.J.B., 1987. Soil moisture measurement by an improved capacitance  
756 technique. Part 1: sensor design and performance. *Journal of Hydrology* 93:67.
- 757 Dempster, A.P., Laird, N.M., Rubin, D.B., 1977. Maximum likelihood from incomplete data via the EM  
758 algorithm. *J.R. Stat. Soc. Ser. B* 39, 1–38.
- 759 Duwig, C., Normand, B., Vauclin, M., Vachaud, G., Green, S.R., Becquer, T., 2003. Evaluation of the  
760 WAVE model for predicting nitrate leaching for two contrasted soil and climate conditions. *Vadose*  
761 *Zone J.* 2, 76–89.
- 762 Gabriel, J. L., Lizaso J.I., Miguel, Q., 2010. Laboratory versus Field Calibration of Capacitance Probes.  
763 *Soil Sci Soc Am J.* 74, 593-601.

- 764 Genereux, D., Slater, E., 1999. Water exchange between canals and surrounding aquifer and wetlands in  
765 the Southern Everglades, USA. *Journal of Hydrology* 219 (1999), 153–168.
- 766 Geweke, J.F., 1977. The dynamic factor analysis of economic time series models. In: Aigner, D.J.,  
767 Goldberger, A.S. (Eds.), *Latent Variables in Socio-economic Models*. North-Holland, Amsterdam,  
768 pp. 365–382.
- 769 Harvey, A.C., 1989. *Forecasting, structural time series models and the Kalman filter*. Cambridge Univ.  
770 Press, New York.
- 771 Kaplan, D., Muñoz-Carpena, R., Wan, Y., Hedgepeth, M., Zheng, F., Roberts, R., Rossmanith, R., 2010a.  
772 Linking river, floodplain, and vadose zone hydrology to improve restoration of a coastal river  
773 impacted by saltwater intrusion. *J. Environ. Quality* 39 (5), 1570–1584. doi:10.2134/jeq2009.0375.
- 774 Kaplan, D., Muñoz-Carpena, R., Ritter, A., 2010b. Untangling complex groundwater dynamics in the  
775 floodplain wetlands of a southeastern U.S. coastal river. *Water Resour. Res.* 46, W08528-10.  
776 doi:10.1029/2009WR009038.
- 777 Kaplan, D., Muñoz-Carpena R., 2011. Complementary effects of surface water and groundwater on soil  
778 moisture dynamics in a degraded coastal floodplain forest. *J. of Hydrol.* 398, 221–234.
- 779 Lütkepohl, H., 1991. *Introduction to multiple time series analysis*. Springer- Verlag, Berlin.
- 780 Márkus, L., Berke, O., Kovács, J., Urfer, W., 1999. Spatial prediction of the intensity of latent effects  
781 governing hydrogeological phenomena. *Environmetrics*. 10, 633-654.
- 782 McDonald, M.G., Harbaugh, A.W., 1988. A modular three-dimensional finite-difference ground-water  
783 flow model. *Techniques of Water Resources Investigations of the United States Geological Survey*,  
784 Book 6, Chapter A1, US Geological Survey, Reston, Virginia.
- 785 Merritt, M.L., 1996. Simulation of the water table altitude in the Biscayne aquifer, Southern Dade  
786 County, Florida, water years 1945-89. *Water-Supply Paper 2458*, US Geological Survey.

- 787 Muñoz-Carpena, R., Ritter, A., Li, Y.C., 2005. Dynamic factor analysis of groundwater quality trends in  
788 an agricultural area adjacent to Everglades National Park. *J. Contam. Hydrol.* 80, 49–70.
- 789 Muñoz-Carpena, R., Ritter, A., Bosch, D.D., Schaffer, B., Potter, T.L., 2008. Summer cover crop impacts  
790 on soil percolation and nitrogen leaching from a winter corn field. *J. Agricultural Water*  
791 *Management.* 95, 633–644.
- 792 Munsell Soil Color Charts., 2000. Revised Edition. Greta G. Macbeth. New Windsor, NY.
- 793 Nash, J.E., Sutcliffe, J.V., 1970. River flow forecasting through conceptual models: Part 1-A. Discussion  
794 of principles. *J. Hydrol.* 10, 282–290.
- 795 Nobel, C.V., Drew, R.R.W., Slabaugh, J.D., 1996. Soil survey of Dade County Area, Florida, U.S.  
796 Department of Agriculture, NRCS Report, Washington, DC.
- 797 Pathak, S. C., 2008. South Florida Water Management District. South Florida Environmental Report  
798 Volume I. Appendix 2-1. Pg. 64. 3301 Gun Club Road, West Palm Beach, FL. Available online  
799 at:[http://my.sfwmd.gov/portal/page/portal/pg\\_grp\\_sfwmd\\_sfer/portlet\\_sfer/tab2236041/v](http://my.sfwmd.gov/portal/page/portal/pg_grp_sfwmd_sfer/portlet_sfer/tab2236041/volume1/v)  
800 [oll\\_table\\_of\\_contents.html](http://my.sfwmd.gov/portal/page/portal/pg_grp_sfwmd_sfer/portlet_sfer/tab2236041/volume1/v).
- 801 Ritter, A., Regalado, C.M., Muñoz Carpena R., 2009. Temporal common trends of topsoil water  
802 dynamics in a humid subtropical forest watershed. *Vadose Zone J.* 8(2), 437–449.
- 803 Ritter A., Muñoz-Carpena, R., 2006. Dynamic factor modeling of ground and surface water levels in an  
804 agricultural area adjacent to Everglades National Park. *J. Hydrol.* 317, 340-354.
- 805 Salas, J.D., 1993. Analysis and modeling of hydrologic time series. p. 19.1–19.72. In D.R. Maidment  
806 (ed.) *Handbook of hydrology.* McGraw-Hill, New York.
- 807 Schaffer, B., 1998. Flooding Responses and Water-use Efficiency of Subtropical and Tropical Fruit Trees  
808 in an Environmentally-sensitive Wetland. *Annals of Botany* 81, 475–481. SFWMD, 2011. Past and  
809 Projected Trends in Climate and Sea Level for South Florida. Hydrologic and Environmental  
810 Systems Modeling. 3301 Gun Club Road West Palm Beach, Florida

- 811 Shumway, R.H., Stoffer D.S., 1982. An approach to time series smoothing and forecasting using the EM  
812 algorithm. *J. Time Ser. Anal.* 3, 253–264.
- 813 Šimůnek, J., van Genuchten, M. Th., Šejna, M., 2008. Development and applications of the HYDRUS  
814 and STANMOD software packages, and related codes, *Vadose Zone J.* 7 (2), 587-600.
- 815 Skinner, C., Bloetscher, F., Pathak, C.S., 2008. Comparison of NEXRAD and Rain Gauge Precipitation  
816 Measurements in South Florida. *J. of Hydrologic Engineering.* 14(3), 248-260.
- 817 U.S. Army Corps of Engineers, and South Florida Water Management District, 2009. Comprehensive  
818 Everglades Restoration Plan: C-111 spreader canal western project: Draft integrated project  
819 implementation report and environmental impact statement.
- 820 USDA Soil Conservation Service. U.S. Department of Agriculture Handbook 18.
- 821 USDA National Agricultural Statistics Service for Miami-Dade County, Florida 2007. Available at:  
822 [http://www.agcensus.usda.gov/Publications/2007/Online\\_Highlights/County\\_Profiles/Florida/cp12](http://www.agcensus.usda.gov/Publications/2007/Online_Highlights/County_Profiles/Florida/cp12)  
823 [086.pdf](http://www.agcensus.usda.gov/Publications/2007/Online_Highlights/County_Profiles/Florida/cp12)
- 824 Vanclooster, M., Viaene, P., Diels, J., Christiaens, K., 1995. WAVE: A mathematical model for  
825 simulating water and agrochemicals in the soil and vadose environment. Reference and user's  
826 manual (release 2.0). Institute for Land and Water Management, Katholieke Universiteit Leuven,  
827 Leuven, Belgium.
- 828 Water Resources Development Act, 2000. PUBLIC LAW 106–541—DEC. 11, 2000.  
829 <http://www.fws.gov/habitatconservation/omnibus/wrda2000.pdf> Retrieved July-23-2010.
- 830 Zou, S., Yu, Y., 1999. A dynamic factor model for multivariate water quality time series with trends. *J. of*  
831 *Hydrology* 178 (1–4), 381–400.
- 832 Zuur, A.F., Ieno, E.N., Smith, G.M., 2007. *Analysing ecological data.* Springer- Verlag, Berlin.
- 833 Zuur, A.F., Pierce, G.J., 2004. Common trends in Northeast Atlantic squid time series. *J. Sea Res.* 52, 57–  
834 72.

- 835 Zuur, A.F., Fryer, R.J., Jolliffe, I.T., Dekker, R., Beukema, J.J., 2003. Estimating common trends in  
836 multivariate time series using dynamic factor analysis. *Environmetrics*. 14 (7), 665–685.